

# Joint species distribution modeling with additive multi-variate Gaussian process priors and heterogeneous data

Jarno Vanhatalo

*Department of Mathematics and Statistics and Organismal and Evolutionary Biology Research Program, University of Helsinki, Helsinki, Finland*

E-mail: [jarno.vanhatalo@helsinki.fi](mailto:jarno.vanhatalo@helsinki.fi)

Marcelo Hartmann

*Department of Mathematics and Statistics, University of Helsinki, Helsinki, Finland*

E-mail: [marcelo.hartmann@helsinki.fi](mailto:marcelo.hartmann@helsinki.fi)

Lari Veneranta

*Natural Resources Institute Finland, Finland*

E-mail: [lari.veneranta@luke.fi](mailto:lari.veneranta@luke.fi)

**Summary.** Species distribution models (SDM) are a key tool in ecological research, conservation and management of natural resources. Two key components of SDMs are, the description for species presence/abundance response along environmental covariates and the spatial random effect that captures deviations from the distribution patterns explained by environmental covariates. Joint species distribution models (JSDMs) include additionally interspecific correlations in both of these components which has been shown to improve their descriptive and predictive performance. However, current JSDMs are restricted to hierarchical generalized linear modeling framework. Their limitation is that parametric models have trouble in locating abrupt changes and change points in abundance due, for example, physical tolerance limits. For example, in aquatic domains, inferring them is particularly important when predicting species distribution in new areas or under scenarios of environmental changes. On the other hand, semiparametric response functions have been shown to improve the predictive performance of SDMs in single species models.

In this work, we propose JSDMs where the responses to environmental covariates are modeled with multivariate additive Gaussian processes. These allow inference for wide range of functional forms and interspecific correlations between the responses. We propose also an efficient approach for inference by utilizing Laplace approximation with a parameterization of the interspecific covariance matrices on the euclidian space. We demonstrate the benefits of our model with two small scale examples and one real world case study. We use cross-validation to compare the proposed model to analogous single species models in interpolation and extrapolation tasks. The proposed model outperforms the single species models in both cases. We also show that the proposed model can be seen as an extension of the current state-of-the-art JSDMs to semiparametric models.

## 1. Introduction

Species distribution models (SDMs) are key tools in the ecologists' toolbox. They have been widely used, among other applications, to study species habitat preferences (Lamster et al., 2006; Austin, 2007; Ovaskainen et al., 2016a), to improve identification and

management of conservation areas and natural resources (Johnston et al., 2015; Cressie & Wikle, 2011) and to evaluate species responses to environmental filtering under climate change scenarios (Clark et al., 2014). The main goal of statistical modelling in these contexts is to use species observations and information on the associated environment to infer the relationship between these two attributes (Gelfand et al., 2006; Latimer et al., 2006). Moreover, when information on environmental characteristics is available from unsampled locations SDMs can be used to predict over these regions to build thematic species distribution maps (Elith & Leathwick, 2009; Gelfand et al., 2006; Miller, 2010; Vanhatalo et al., 2012; Kallasvuo et al., 2017).

Hence, species distribution modeling is directly related to a specification of species' responses to environmental factors (Latimer et al., 2006). This is traditionally done using generalized linear or additive models (Guisan et al., 2002; Gelfand et al., 2006; Elith & Leathwick, 2009; Ovaskainen et al., 2017) which model each species separately and cannot account for species interactions nor shared responses to their environment. However, when predicting spatial distribution patterns, species interaction with other species is potentially as important factor as its response to environmental variation. Moreover, in many practical situations, data from species can be patchy or scarce in which case sharing information between species can significantly improve models' predictive performance (Ovaskainen & Soininen, 2011; Clark et al., 2014; Hui et al., 2013; Taylor-Rodríguez et al., 2016; Hartmann et al., 2017). For these reasons, joint species distribution models (JSDM) have gained increasing attention in recent years (Warton et al., 2015).

For example, Ovaskainen et al. (2017) introduced the hierarchical modeling of species communities (HMSC) framework which includes detailed description of interspecific correlations in covariate responses as well as spatial random effects. Pollock et al. (2014) proposed the multivariate probit regression model from Chib & Greenberg (1998) to describe geographical co-occurrence patterns between frogs and eucalypt trees in Australia and Clark et al. (2014) used JSDMs to infer spatial distribution richness and loss of species under climate change scenarios. Dunstan et al. (2013) and Hui et al. (2013) introduced species archetype modeling where species' responses to the environment are clustered into few archetype (generalized linear) models.

Current JSDMs rely on the classical framework of hierarchical generalized linear models (GLMs). Even though this approach allows flexible modelling by describing the randomness of response variables with different probabilistic models (Nelder & Wedderburn, 1972), it is still limited by its parametric assumptions (Bickel & Doksum, 1977). Hence, it may fail to describe a species' response to the large range of environmental conditions (Vanhatalo et al., 2012; Kallasvuo et al., 2017). Here, we propose to construct JSDMs by assuming a semiparametric model represented with Gaussian processes (GP) (Vanhatalo et al., 2012; Rasmussen & Williams, 2006). GPs are flexible semiparametric regression models where the regression function is estimated without imposition of restrictive parametric assumptions about its form (O'Hagan, 1978). Our models couple together the main properties of semiparametric single species models (Vanhatalo et al., 2012; Golding & Purse, 2016) and generalized linear model based joint species distribution models (Pollock et al., 2014; Ovaskainen et al., 2017). In the first stage, we assume that measurements are conditionally independent given an underlying mul-

tivariate latent process. In the second stage, the latent multivariate process describes the species specific responses to abiotic environment and includes spatial random effect that captures the spatial structure in the data that is not described by covariates.

The novel unique contributions in our work are the following. Firstly, instead of hierarchical linear formalism we model the species responses to environmental covariates through additive multivariate Gaussian processes (GP). This allows us to capture the wide range of nonlinear responses and to share information about these responses between species. Secondly, due to the hierarchical model structure, the methodology can accommodates several kinds of outcome variables altogether by assigning different types of probabilistic models for different types of measurements. This is important, since it will allow us to exploit different types of measurements which commonly arise in real-case scenarios of multiple species surveys. Our presentation focus in the mostly used probabilistic models in practice, the Binomial (Bernoulli) and Negative-Binomial (Poisson). We also propose an efficient computational approach build around Laplace method and expectation propagation algorithms (Golding & Purse, 2016). Lastly, we present a structured cross-validation scheme to validate and compare models' performance in different kinds of prediction tasks.

This paper is organized as follows. In Section 2 we introduce a motivating case study. In section 3, we introduce the additive multivariate Gaussian process and in Section 4 we discuss its predictive properties and introduce the computational methods for inference. In Section 5, we illustrate the basic properties of the model through two simple examples and introduce the specific case study model. In Section 6 we present the case study results and we end by discussion and conclusions in Section 7.

## 2. Motivating case study: coastal species distributions in the Gulf of Bothnia

As a motivating example for our work, we will consider a case study on spring distribution of four fish species and three types of algae or macrovegetation on the coastal region of the Gulf of Bothnia in the northern Baltic Sea. The Gulf of Bothnia is a brackish water basin between Sweden and Finland covering an area of approximately  $600 \times 120$  km. It hosts wide range of environmental conditions and its coastal areas play a central role in the ecosystem (Veneranta et al., 2013; Lundeberg et al., 2009). For example, many Baltic fish stocks are dependent on the coastal regions for their reproduction (Veneranta et al., 2011, 2013; Vanhatalo et al., 2012; Kallasvuo et al., 2017). Coastal zones are also the most sensitive regions of the Baltic sea to both natural variation and anthropogenic pressures (Helsinki Comission, 2009; Borja et al., 2003), for which reason these areas are of central importance for conservation and marine spatial planning. Hence, there is need for detailed knowledge on the distribution of coastal species and predictions concerning their response to environmental changes.

### 2.1. Case study species and data

The studied fish species are the juvenile or adult threespine-stickleback (*Gasterosteus aculeatus*) and ninespine-stickleback (*Pungitius pungitius*) as well as larvae of whitefish (*Coregonus lavaretus*) and vendace (*Coregonus albula*). Both whitefish and vendace are commercially important species, whereas the sticklebacks are the essential but not

very well known part of ecosystem in the Northern Baltic Sea (Bergström et al., 2015). The studied vegetation and algae are treated in functional group level and comprise of diatomous and filamentous algae and macro-vegetation. These are the dominating groups of benthic vegetation in shallowest shores where larvae of Coregonids (whitefish and vendace) occur at early developmental stages. In the scale of Gulf of Bothnia, their occurrence also reflects the salinity, nutrient balance and wind exposure of studied area (Veneranta et al., 2013).

The studied species reflect the large scale environmental gradients and also the changes that have happened in the Baltic Sea status in last decades. Sticklebacks in the Baltic Sea use the shallow coastal zone for reproduction (Bergström et al., 2015) and high abundances of sticklebacks in the Baltic Sea have been positively correlated with filamentous algal blooms (Eriksson et al., 2009, 2012). In opposite to that, Coregonids prefer more oligotrophic waters (Veneranta et al., 2013). Whitefish and vendace reproduce in stony reefs and islets of Baltic Sea in late autumn and the larvae hatch at ice break-up in spring. After winter, in sheltered areas the overwintering reeds (*Phragmites australis*) dominate the macrovegetation, forming structure and shelter to shallow shoreline. Diatomous algae consist of several epiphytic species that have an early spring bloom at ice break up and settle rapidly over bottom when light and water temperature increase (Busse & Snoeijs, 2002). Filamentous algae in this study consist mostly of *Pitayella* sp. It is a fast growing annual species that dominates the exposed shores in early spring at Baltic Sea (Rönnberg & Bonsdorff, 2004).

The data collection was conducted by dividing the whole study area (Gulf of Bothnia) into sampling subareas. Within each subarea, data were collected at several sampling sites distributed so that they covered the range of *a priori* most important environmental covariates in that subarea. The species data used in this work comprise of 160 distinct sampling sites from years 2009 and 2010 (Figure 1). In 70 sites (2010 data) all species have been sampled and the rest of the sites comprise samples only for the fishes (Figure 1). Fish samples comprise the number of observed fish together with information on the sampling effort at each site. The effort was measured as the volume of water (m<sup>3</sup>) sampled by the fishing net (see Veneranta et al., 2013; Vanhatalo et al., 2012). For plant data, the bottom was photographed at 5-13 locations at depth of 30 cm within a distance of 2 m and parallel to shore line. The presence/absence of a species was recorded at 16 uniformly distributed points in all these photographs. The plants studied here can grow over each others so that presence of one plant at a spatial location does not exclude the presence of other plants. The whitefish and vendace data were previously analyzed by Veneranta et al. (2013) and Vanhatalo et al. (2012) but the data on other species are unpublished.

## 2.2. Environmental covariates

The study area hosts rich variety of different environmental conditions. Coastal areas are affected by inflows from land as well as shallow and complex topography. In addition, in the scale of GoB, there is a gradient in river influence, salinity, temperature and length of ice cover period from north to south. We used seven real-valued covariates and one categorical abiotic environmental covariate that were available throughout the study area as raster maps with resolution of 300 m × 300 m. These are summarized in table

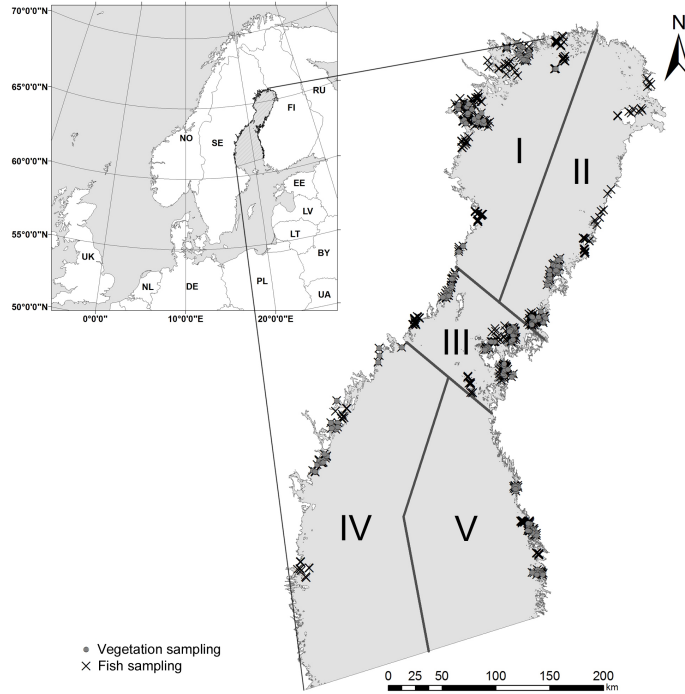


**Fig. 1.** The study region, Gulf of Bothnia, and locations for species data. The region is divided into five subregions (I-V) to be used in cross-validation. The environmental conditions (described by the environmental covariates) are heterogeneous between these regions (Veneranta et al., 2013) which allows to test models' extrapolation performance.

1 and described in detail and motivated by Veneranta et al. (2013). Due its fresh water origin vendace is *a priori* sensitive to even small changes in salinity levels experienced in the Gulf of Bothnia whereas the other species respond to salinity only in the Baltic Sea scale. Hence, we used all covariates only for vendace but excluded the winter salinity from other species. Each sample location was attached with environmental covariates corresponding to the raster cell where the sample location falls in.

### 3. Additive multivariate Gaussian processes

#### 3.1. Hierarchical multivariate species distribution model

We start our model building following the generic hierarchical structure similar to, e.g., Wikle (2003), Cressie & Wikle (2011) and Banerjee et al. (2015)

$$\begin{aligned}
 [\text{data} | \text{process, parameters}] &: \pi_Y(\mathbf{y}(\mathbf{x}, \mathbf{s}) | \mathbf{f}(\mathbf{x}, \mathbf{s}), \boldsymbol{\eta}) \\
 [\text{process} | \text{parameters}] &: \pi_f(\mathbf{f}(\mathbf{x}, \mathbf{s}) | \boldsymbol{\theta}) \\
 [\text{parameters}] &: \pi(\boldsymbol{\eta}, \boldsymbol{\theta})
 \end{aligned} \tag{1}$$

**Table 1.** Environmental covariates used in the case study and their resolution.

Variable	Description	Resolution [m]
Opennes	The average opennes and exposure to winds	300
Distance to deep	Distance to 20 m depth curve	200
Sandy bottom index	Area weighted distance to the sandy shores	90
Ice breakup week	The end date (weeks) of ice cover in 2009	1852
Chlorophyl-a	Chlorophyl-a concentration	1852
River	Distance to the nearest river mouth	150
Bottom class	Bottom classification to 6 categories	200
Winter salinity	Length of icewinter	10,000

where the first layer of hierarchy is the probabilistic model which defines the conditional distribution for multivariate data  $\mathbf{Y}(\mathbf{x}, \mathbf{s})$ , at spatial location  $\mathbf{s}$  with associated covariates  $\mathbf{x}$ , given the model parameters  $\boldsymbol{\eta}$  and the multivariate latent process  $\mathbf{f}(\mathbf{x}, \mathbf{s})$ . The second layer defines the prior distribution for the latent process given the process parameters  $\boldsymbol{\theta}$ , and the third layer defines the prior distribution for all unknown parameters.

Let  $j \in \mathcal{J} = \{1, \dots, J\}$  be the species index set and  $J$  the total number of species in the study. Denote by  $\mathbf{Y}(\mathbf{x}, \mathbf{s})^T = [Y_1 \dots Y_J]$  the  $J$ -variate random vector with components  $Y_j = Y_j(\mathbf{x}_j, \mathbf{s})$  related to the  $j^{\text{th}}$  species at spatial location  $\mathbf{s}^T = [s_1 \ s_2]$  under the influence of environmental covariates  $\mathbf{x}_j^T = [x_{j,1} \dots x_{j,c_j}]$  where  $c_j$  is the number of environmental covariates for the species  $j$ . We denote by  $\mathbf{x}$  the full vector of covariates and  $\mathcal{X}$  the covariate space. The species specific covariates  $\mathbf{x}_j$  are subvectors of  $\mathbf{x}$  such that  $\mathbf{x}_j \in \mathcal{X}_j$  where  $\mathcal{X}_j \subset \mathcal{X}$  and  $\mathcal{X}_j$  is  $c_j$ -dimensional. Here, we assume that given a multivariate latent process  $\mathbf{f}(\mathbf{x}, \mathbf{s}) = [f_1(\mathbf{x}_1, \mathbf{s}) \dots f_J(\mathbf{x}_J, \mathbf{s})]^T : \mathcal{X} \times \mathbb{R}^2 \rightarrow \mathbb{R}^J$ , the probabilistic model for  $\mathbf{Y} = \mathbf{Y}(\mathbf{x}, \mathbf{s})$  factorizes as follows

$$\pi_{\mathbf{Y}}(\mathbf{y}(\mathbf{x}, \mathbf{s}) | \mathbf{f}(\mathbf{x}, \mathbf{s}), \boldsymbol{\eta}) = \prod_{j=1}^J \pi_{Y_j}(y_j | f_j, \eta_j) \quad (2)$$

where  $f_j = f_j(\mathbf{x}_j, \mathbf{s})$  is fixed but an unknown realization of the  $j^{\text{th}}$  process with covariates  $\mathbf{x}_j$  at the spatial location  $\mathbf{s}$ .  $\eta_j$  is the vector of parameters of the probabilistic model  $\pi_{Y_j}$  for the species  $j$  and  $\boldsymbol{\eta} = [\eta_1 \dots \eta_J]^T$ . Notice that, we allow two random variables  $Y_j$  and  $Y_{j'}$  to follow distributions which belong to the same family, say  $\{\pi(\cdot | \eta_j) : \eta_j \in \Xi\}$  where  $\Xi$  is a parametric space. However, in this work, we consider distinct parameters  $\eta_j \neq \eta_{j'} \in \Xi$  if not otherwise stated.

In general any probabilistic model for data could be used and the observation models should be chosen according to the assumed sampling process. In this work, however, we will consider in detail the Binomial (or Bernoulli) and the Negative-Binomial (or Poisson) models which are common in SDMs and used in our case study (Section 2). Moreover, these models can be seen as observation models resulting from inhomogenous point process model for the species abundance (Gelfand et al., 2006; Warton & Shepherd, 2010; Illian et al., 2013; Yuan et al., 2016). The Binomial model is given by,

$$\pi_{Y_B}(y | f(\mathbf{x}, \mathbf{s}), z_B(\mathbf{s})) = \binom{z_B(\mathbf{s})}{y} p(f(\mathbf{x}, \mathbf{s}))^y [1 - p(f(\mathbf{x}, \mathbf{s}))]^{z_B(\mathbf{s})-y} I_{\{0, \dots, z_B(\mathbf{s})\}}(y) \quad (3)$$

where  $z_B(\mathbf{s})$  is the total number of observations at location  $\mathbf{s}$  and  $p(f(\mathbf{x}, \mathbf{s}))$  is the success

probability, which will be chosen to be the logit here. The Negative-Binomial model is given with the following parameterization

$$\pi_{Y_N}(y|f(\mathbf{x}, \mathbf{s}), z_N(\mathbf{s}), r) = \frac{\Gamma(r+y)}{y!\Gamma(r)} \left( \frac{r}{r+m(\mathbf{x}, \mathbf{s})} \right)^r \left( \frac{m(\mathbf{x}, \mathbf{s})}{r+m(\mathbf{x}, \mathbf{s})} \right)^y I_{\mathbb{N}_0}(y) \quad (4)$$

where  $m(\mathbf{x}, \mathbf{s}) = z_N(\mathbf{s}) \exp[f(\mathbf{x}, \mathbf{s})]$  is the expected value of  $Y_N|f(\mathbf{x}, \mathbf{s}), z_N(\mathbf{x}), r$ . The predictor function  $f(\cdot)$  corresponds to the logarithm of the species relative density and  $z_N(\mathbf{s})$  is the sampling effort in location  $\mathbf{s}$ . For this particular parameterization we have that  $V(Y_N|f(\mathbf{x}, \mathbf{s}), z_N(\mathbf{x}), r) = m(\mathbf{x}, \mathbf{s}) + m(\mathbf{x}, \mathbf{s})^2/r$ , where  $r$  is the over-dispersion parameter. Increasing  $r$  decreases the variance and in the limit of  $r \rightarrow \infty$ , the model becomes the Poisson distribution.

### 3.2. Univariate additive latent Gaussian process

First, we assume that marginally for any species  $j$ , the process model is given by

$$f_j(\mathbf{x}_j, \mathbf{s}) = \beta_{j,0} + h_j(\mathbf{x}_j) + \varepsilon_j(\mathbf{s}) \quad (5)$$

where  $\beta_{j,0}$  is the offset weight with distribution  $\beta_{j,0}|\sigma_{j,0}^2 \sim \mathcal{N}(0, \sigma_{j,0}^2)$  and  $h_j : \mathcal{X}_j \rightarrow \mathbb{R}$  is a *predictor function* of environmental covariates. The predictor function is assumed to be additive over the covariates,  $h_j(\mathbf{x}_j) = \sum_{r=1}^{c_j} h_{j,r}(x_{j,r})$ , and each additive term is given an independent zero mean Gaussian process (GP) prior, so that

$$h_j(\mathbf{x}_j) | \boldsymbol{\theta}_j \sim \mathcal{GP} \left( 0, \sum_{r=1}^{c_j} k_{h_{j,r}}(x_{j,r}, x'_{j,r}; \boldsymbol{\theta}_{j,r}) \right) \quad (6)$$

where  $k_{h_{j,r}}(x_{j,r}, x'_{j,r}; \boldsymbol{\theta}_{j,r}) = \text{Cov}(h_{j,r}(x_{j,r}), h_{j,r}(x'_{j,r}) | \boldsymbol{\theta}_{j,r})$  is a covariance function with parameter  $\boldsymbol{\theta}_{j,r}$  and  $\boldsymbol{\theta}_j = [\boldsymbol{\theta}_{j,1}^T \cdots \boldsymbol{\theta}_{j,c_j}^T]^T$ . For example, with  $k_{h_{j,r}}(x_{j,r}, x'_{j,r}; \boldsymbol{\theta}_{j,r}) = x_{j,r} x'_{j,r} \sigma_{j,r}^2$  and  $\theta_{j,r} = \sigma_{j,r}^2$ , the predictor function corresponds to linear model  $h_{j,r}(x_{j,r}) = x_{j,r} \beta_{j,r}$  where  $\beta_{j,r} \sim N(0, \sigma_{j,r}^2)$  (Rasmussen & Williams, 2006). With other choices of covariance functions we can model non-linear responses in which case the model can be seen as an alternative to the traditional generalized additive models (GAMs, Hastie & Tibshirani, 1986). The general form of an additive GP prior would include also joint effects of covariates (Duvenaud et al., 2011) but this is not considered here.

The term  $\varepsilon_j(\mathbf{s})$  is a spatial Gaussian process,

$$\varepsilon_j(\mathbf{s}) | \sigma_j^2, \boldsymbol{\ell}_j \sim \mathcal{GP}(0, k_{\varepsilon_j}(\mathbf{s}, \mathbf{s}'; \boldsymbol{\ell}_j, \sigma_j^2)) \quad (7)$$

where  $k_{\varepsilon_j}(\mathbf{s}, \mathbf{s}'; \boldsymbol{\ell}_j, \sigma_j^2)$  is a spatial covariance function with variance  $\sigma_j^2$  and range parameter  $\boldsymbol{\ell}_j$ . When we consider independent models for each species, that is the traditional single species SDMs (SSDMs), the processes  $h_{j,r}$  and  $\varepsilon_j$  are mutually independent among all species. Until this point, the model outlined this far is similar to the GP based species distribution models used by, e.g., Vanhatalo et al. (2012), Kallasvuo et al. (2017) and Golding & Purse (2016). Next, we introduce models which consider dependency.

### 3.3. Additive multivariate Gaussian process priors

In order to account for possible species interdependence, we first include spatial species interaction into the model through the linear model of coregionalization (LMC) (Mardia & Goodall, 1993; Gelfand et al., 2004). Write  $\boldsymbol{\varepsilon}(\mathbf{s})^T = [\varepsilon_1(\mathbf{s}) \cdots \varepsilon_J(\mathbf{s})]$  and assume that  $\boldsymbol{\varepsilon}(\mathbf{s})$  has LMC covariance structure with species specific correlation functions  $\tilde{k}_{\epsilon_j}(\cdot, \cdot; \boldsymbol{\ell}_j) = k_{\epsilon_j}(\cdot, \cdot; \sigma_j^2 = 1, \boldsymbol{\ell}_j)$ . Then the covariance structure of the LMC with interspecies spatial dependence is given by,

$$\text{Cov}(\varepsilon_j(\mathbf{s}), \varepsilon_{j'}(\mathbf{s}') | \Sigma_\epsilon, \boldsymbol{\ell}) = \sum_{l=1}^J u_{\epsilon,l}(j, j') \tilde{k}_{\epsilon_l}(\mathbf{s}, \mathbf{s}'; \boldsymbol{\ell}_l) \quad (8)$$

with  $\boldsymbol{\ell}^T = [\boldsymbol{\ell}_1^T \cdots \boldsymbol{\ell}_J^T]$  and  $u_{\epsilon,l}(j, j')$  the entry  $(j, j')$  of  $U_{\epsilon,l} = L_{\epsilon,l} L_{\epsilon,l}^T$  where  $L_{\epsilon,l}$  is the  $l^{th}$  column of the Cholesky decomposition  $L_\epsilon$  of the coregionalization matrix  $\Sigma_\epsilon$ , that is matrix of interspecific correlations between spatial GPs. Hence, the vector-valued latent process  $\mathbf{f}(\mathbf{x}, \mathbf{s})^T = [f_1(\mathbf{x}_1, \mathbf{s}) \cdots f_J(\mathbf{x}_J, \mathbf{s})]$  unconditional on  $\beta_{1,0}, \dots, \beta_{J,0}$  follows a multivariate Gaussian process which we denote as

$$\mathbf{f}(\mathbf{x}, \mathbf{s}) | \Lambda_1 \sim \mathcal{MGP}\left(\mathbf{0}, \Sigma_0 + \sum_{r=1}^c k_{h_r}(\mathbf{x}_r, \mathbf{x}'_r; \boldsymbol{\theta}) + \sum_{j=1}^J \tilde{k}_{\epsilon_j}(\mathbf{s}, \mathbf{s}'; \boldsymbol{\ell}_j) U_{\epsilon,j}\right) \quad (9)$$

where  $\Lambda_1 = (\Sigma_0, \Sigma_\epsilon, \boldsymbol{\theta}, \boldsymbol{\ell})$ ,  $\Sigma_0 = \text{diag}(\sigma_{1,0}^2, \dots, \sigma_{J,0}^2)$ ,  $\boldsymbol{\theta}^T = [\boldsymbol{\theta}_1^T \cdots \boldsymbol{\theta}_J^T]$  and  $k_{h_r}(\mathbf{x}_r, \mathbf{x}'_r; \boldsymbol{\theta}) = \text{diag}(k_{h_{1,r}}(x_{1,r}, x'_{1,r}; \boldsymbol{\theta}_{1,r}), \dots, k_{h_{J,r}}(x_{J,r}, x'_{J,r}; \boldsymbol{\theta}_{J,r}))$ . If the predictor functions,  $h_{j,r}$ , were linear, the prior (9) would correspond to traditional multivariate spatial model with independent linear effects and spatial LMC (Gelfand et al., 2004).

We extend (9) to an *additive multivariate Gaussian process prior* where the dependence between the species specific additive predictor functions is modeled through LMC. We demonstrate this with a multivariate Gaussian process model where the set of covariates is equal for all species, that is,  $\dim(\mathcal{X}_j) = c$  and  $\mathbf{x}_j = \mathbf{x}$  for all  $j$ . Then the model is written as

$$\mathbf{f}(\mathbf{x}, \mathbf{s}) | \Lambda_2 \sim \mathcal{MGP}\left(\mathbf{0}, \Sigma_0 + \sum_{r=1}^c \sum_{j=1}^J \tilde{k}_{h_{j,r}}(x_r, x'_r; \boldsymbol{\theta}_{j,r}) U_{h_{j,r},j} + \sum_{j=1}^J \tilde{k}_{\epsilon_j}(\mathbf{s}, \mathbf{s}'; \boldsymbol{\ell}_j) U_{\epsilon,j}\right) \quad (10)$$

where  $\Lambda_2 = (\Lambda_1, \Sigma_{h_1}, \dots, \Sigma_{h_c})$  and  $\Sigma_{h_r}$  is the interspecific covariance matrix between the species specific predictor functions of  $r^{th}$  covariate,  $\tilde{k}_{h_{j,r}}(\cdot, \cdot; \boldsymbol{\theta}_{j,r})$  is a correlation function related to the predictor function  $h_{j,r}$ ,  $U_{h_{j,r},j} = L_{h_{j,r},j} L_{h_{j,r},j}^T$  and  $L_{h_{j,r},j}$  is the  $j^{th}$  column of the Cholesky decomposition  $L_{h_r}$  of  $\Sigma_{h_r}$ . When the set of covariates is not the same for all species, covariate specific predictive functions are correlated only between species that share those same covariates.

A JSDM with multivariate GP prior (10) can be interpreted as extension of GP based SSDMs (Vanhatalo et al., 2012; Golding & Purse, 2016) to joint species modeling similarly as done with the generalized linear model based JSDMs (Ovaskainen et al., 2017). The enhanced inferential ability of the multivariate additive GP compared to univariate GP models lies in its capability to infer similarity (dissimilarity) in species specific

responses to covariates and in the spatial random effect. The similarity/dissimilarity of responses of two species  $j$  and  $j'$  along a covariate  $r$  is indicated by a positive/negative value for correlation and hence, examining the LMC covariance matrices,  $\Sigma_{h_r}$ , can provide new insight to species to species associations.

The model formulation will be finalized by defining the covariance functions for the GP models and the prior distributions for the hyperparameters. Next we define the prior for coregionalization covariance matrices but define the covariance functions and rest of the priors in Section 5 together with our case study application.

### 3.4. Marginally uniform priors for correlation parameters of LMC components

A standard choice for prior for correlation matrices is the inverse Wishart distribution. However, if there is no prior information on interspecific correlations, we follow Hartmann et al. (2017) and suggest to use marginally uniform priors for the LMC covariance matrices  $\Sigma_\epsilon$  and  $\Sigma_{h_r}$ . These can be achieved by the distribution of Barnard et al. (2000) and Tokuda et al. (2012). Let  $\mathcal{P}$  be a correlation matrix with elements  $\rho_{j,j'}$ . A prior distribution that is marginally noninformative for the correlations, that is, the marginal distribution for every correlation parameter  $\rho_{j,j'}$  is uniform over  $(-1, 1)$  is achieved with the distribution

$$\pi(\mathcal{P} | v) = \frac{\Gamma(\frac{v}{2})^J}{\Gamma_J(\frac{v}{2})} |\mathcal{P}|^{\frac{1}{2}(v-1)(J-1)-1} \prod_{j=1}^J |\mathcal{P}_{jj}|^{-\frac{v}{2}} \mathbb{1}_{(0,\infty)}(\det \mathcal{P}) \quad (11)$$

when  $v = J-1$ . Here,  $\Gamma_J(\cdot)$  is the multivariate gamma function,  $|\mathcal{P}_{jj}|$  is the determinant of a submatrix  $\mathcal{P}_{jj}$  which is obtained by removing the  $j^{th}$  column and  $j^{th}$  row of  $\mathcal{P}$ . When  $v$  increases, the probability density (11) becomes increasingly concentrated around the origin.

## 4. Posterior inference and predictive properties of multivariate additive GPs

Given a set of species observations at locations  $\mathbf{s}_{i_j}$ ,  $i_j = 1, \dots, n_j$ , respectively for each species  $j = 1, \dots, J$ , the likelihood can be written as

$$\pi(\mathbf{y} | \mathbf{f}, \boldsymbol{\eta}) = \prod_{j=1}^J \prod_{i_j=1}^{n_j} \pi_j(y_{j,i_j} | \mathbf{f}_{j,i_j}, \eta_j) \quad (12)$$

where  $y_{j,i_j}$  is the  $i_j$ 'th observation of species  $j$  at the  $i_j$ 'th spatial location  $\mathbf{s}_{i_j}^T$  associated with a set of covariates  $\mathbf{x}_{i_j} \in \mathcal{X}_j$ . The observed vector  $\mathbf{y} = [\mathbf{y}_1^T \cdots \mathbf{y}_J^T]^T$  with  $\mathbf{y}_j^T = [y_{j,1} \cdots y_{j,n_j}]$  collects all the species observations and  $\mathbf{f} = [\mathbf{f}_1^T \cdots \mathbf{f}_J^T]^T$ , where  $\mathbf{f}_j^T = [\mathbf{f}_{j,1} \cdots \mathbf{f}_{j,n_j}]$ , collects the corresponding latent variables. Hence, the likelihood factorizes over the latent variables and the inference can be done similarly as with univariate Gaussian process models. Markov chain Monte Carlo (MCMC) would provide exact answers in the limit of large sample size but deterministic approximations such as Laplace approximation or expectation propagation algorithm have also proved to provide accurate approximate inference for univariate GP models with much lower computational

time requirements (Nickisch & Rasmussen, 2008; Rue & Marino, 2009; Vanhatalo et al., 2010; Golding & Purse, 2016). In order to study the properties of the model, we will examine the Laplace approximation for the posterior of latent variables conditional on the hyperparameters.

#### 4.1. Posterior predictive inference conditional on hyperparameters

##### 4.1.1. Posterior of latent variables

The Laplace's method approximates the conditional posterior of the latent function values  $\mathbf{f}_* = \mathbf{f}(\mathbf{s}_*, \mathbf{x}_*)$  at the spatial location  $\mathbf{s}_*$  with covariates  $\mathbf{x}_*$  as†

$$\pi(\mathbf{f}_* | \mathbf{y}, \boldsymbol{\eta}, \Lambda) \approx \mathcal{N}(\mathbf{f}_* | C_{*,\mathbf{f}} C^{-1} \hat{\mathbf{f}}, C_* - C_{*,\mathbf{f}} (C^{-1} + \mathbf{W})^{-1} C_{\mathbf{f},*}) \quad (13)$$

where  $\hat{\mathbf{f}}$  is the (conditional) maximum a posterior (MAP) estimate of latent variables,

$$\hat{\mathbf{f}} = \arg \max_{\mathbf{f} \in \mathbb{R}^{\sum_j n_j}} \sum_{j=1}^J \sum_{i_j=1}^{n_j} \log \pi_j(y_{j,i_j} | \mathbf{f}_{j,i_j}, \eta_j) + \log \mathcal{N}(\mathbf{f} | \mathbf{0}, C) \quad (14)$$

and  $\mathbf{W}$  is the Hessian matrix of the negative log-likelihood function evaluated at  $\hat{\mathbf{f}}$ . Here,  $C$  is the prior covariance matrix of  $\mathbf{f}$ ,  $C_{*,\mathbf{f}}$  is the (prior) covariance matrix between elements of  $\mathbf{f}_*$  and  $\mathbf{f}$ .  $C_*$  is the prior covariance of  $\mathbf{f}_*$ . In case of multivariate additive Gaussian process (10) the prior covariance matrix is given by

$$\begin{aligned} C = & \begin{bmatrix} \sigma_0^2 \mathbf{J}_{n_1} & \cdots & 0 \\ \vdots & \ddots & \vdots \\ 0 & \cdots & \sigma_0^2 \mathbf{J}_{n_J} \end{bmatrix} + \sum_{r=1}^c \sum_{j=1}^J \begin{bmatrix} u_{h_r,j}(1,1)\{\tilde{K}_{h_{j,r}}\}_{1,1} & \cdots & u_{h_r,j}(1,J)\{\tilde{K}_{h_{j,r}}\}_{1,J} \\ \vdots & \ddots & \vdots \\ u_{h_r,j}(J,1)\{\tilde{K}_{h_{j,r}}\}_{J,1} & \cdots & u_{h_r,j}(J,J)\{\tilde{K}_{h_{j,r}}\}_{J,J} \end{bmatrix} \\ & + \sum_{j=1}^J \begin{bmatrix} u_{\epsilon,j}(1,1)\{\tilde{K}_{\epsilon_j}\}_{1,1} & \cdots & u_{\epsilon,j}(1,J)\{\tilde{K}_{\epsilon_j}\}_{1,J} \\ \vdots & \ddots & \vdots \\ u_{\epsilon,j}(J,1)\{\tilde{K}_{\epsilon_j}\}_{J,1} & \cdots & u_{\epsilon,j}(J,J)\{\tilde{K}_{\epsilon_j}\}_{J,J} \end{bmatrix} \end{aligned} \quad (15)$$

where  $\mathbf{J}_n$  is an  $n \times n$  matrix full of ones  $u_{\epsilon,l}(j,j')$  and  $u_{h_r,l}(j,j')$  are the entry  $(j,j')$  of  $U_{\epsilon,l}$  and  $U_{h_r,l}$  (see (8)), and  $\{\tilde{K}_{\epsilon_j}\}_{j,j'}$  and  $\{\tilde{K}_{h_{l,r}}\}_{j,j'}$  are the correlation matrices between species  $j$  and  $j'$  at their observations sites calculated with correlation functions  $\tilde{k}_{\epsilon,l}(\cdot, \cdot; \boldsymbol{\ell}_l)$  and  $k_{h_{l,r}}(\cdot, \cdot | \boldsymbol{\theta}_{l,r})$  respectively. The other prior covariances have the same structure. Note, if all the species are observed at equal numbers at same locations, then the covariance matrix can be written with Kronecker product similarly as done with LMC models by Mardia & Goodall (1993) and Gelfand et al. (2004), so that  $C = \Sigma_0 \otimes J_n + \sum_{r=1}^c \sum_{j=1}^J U_{h_{j,r},j} \otimes \tilde{K}_{h_{j,r}} + \sum_{j=1}^J U_{\epsilon,j} \otimes \tilde{K}_{\epsilon_j}$  where  $n = n_j$  for all  $j = 1, \dots, J$ . Since, in general, the second and third term of  $C$  are full matrices, it can be seen from (13) and (14) that the posterior of  $\mathbf{f}$  and the posterior predictive distribution of  $\mathbf{f}_*$  are affected by observations of all species at any spatial location.

†In case of Gaussian observation model, this equals to the true posterior density of  $\mathbf{f} | \mathbf{y}, \boldsymbol{\eta}, \Lambda$ .

#### 4.1.2. The marginal posterior of additive terms

Conditional on hyperparameters, the marginal posterior of any additive latent function is analogous to (13) but  $C_*$  and  $C_{*,f}$  are constructed only by the covariance functions corresponding to the predicted component. For example, if we predict  $h_{j,r}(\mathbf{s}_*, \mathbf{x}_*)$ , we replace  $C_{*,f}$  in (13) with

$$C_{*,h_{j,r}} = \sum_{l=1}^J \left[ u_{h_r,l}(j, 1) \{ \tilde{K}_{h_{l,r}} \}_{j,1}, \dots, u_{h_r,l}(j, J) \{ \tilde{K}_{h_{l,r}} \}_{j,J} \right].$$

However, in case of the traditional LMC (9) only the spatial random effects are correlated between species whereas the predictor functions are not. That is,  $\Sigma_{h_r}$  is diagonal for all  $r$  so that  $u_{h_r,l}(j, j') = \sigma_l^2$  if  $l = j = j'$  and zero otherwise. Hence, the second terms of (15) and  $C_{*,h_{j,r}}$  will be block diagonal and there is no information exchange between species specific predictor functions. In case of univariate GP prior all the terms in (15) are block diagonal so that (13) reduces to  $J$  independent Gaussian distributions and there is no information exchange among species at all. Hence, the predictive performance of the univariate GP and the two multivariate GP models are very different. This is illustrated in section 5.

#### 4.1.3. The (marginal) posterior expectation and variance for new observations

When predicting species occurrence probability or abundance, we need to marginalize over the posterior of the latent variables. The posterior expectation and variance for the new outcome for species  $j$  at the new point  $(\mathbf{x}_*, \mathbf{s}_*)$  conditional on the hyperparameters and data, can be obtained as

$$\begin{aligned} \mathbb{E}[Y_j(\mathbf{x}_*, \mathbf{s}_*) | \mathbf{y}, \boldsymbol{\eta}, \Lambda] &= \mathbb{E}[\mathbb{E}(Y_j(\mathbf{x}_*, \mathbf{s}_*) | f_j(\mathbf{x}_*, \mathbf{s}_*), \mathbf{y}, \boldsymbol{\eta}, \Lambda)] \\ \mathbb{V}[Y_j(\mathbf{x}_*, \mathbf{s}_*) | \mathbf{y}, \boldsymbol{\eta}, \Lambda] &= \mathbb{E}[\mathbb{V}(Y_j(\mathbf{x}_*, \mathbf{s}_*) | f_j(\mathbf{x}_*, \mathbf{s}_*), \mathbf{y}, \boldsymbol{\eta}, \Lambda)] + \\ &\quad \mathbb{V}[\mathbb{E}(Y_j(\mathbf{x}_*, \mathbf{s}_*) | f_j(\mathbf{x}_*, \mathbf{s}_*), \mathbf{y}, \boldsymbol{\eta}, \Lambda)] \end{aligned} \quad (16)$$

When the probabilistic model for species  $j$  is assumed to be the Negative-Binomial or Binomial model with logistic link function (3) we can find either an exact result or an analytical approximation for these expectations and variances. These are given in the 7.3. These solutions speed up the predictive calculations considerably compared to numerically integrating  $f$  over  $\mathbb{R}$ .

#### 4.1.4. Conditional scenario predictions

In some applications, one might be interested in scenario predictions conditional on changes in species composition. For example, one might be interested in how removing from or introducing specific species into an area would affect other species. In our case study setting, we could be interested in, for example, effects of management actions that would clean filamentous algae from the shoreline. Such scenario predictions would be naturally tackled with predictive causal inference (Lindley, 2002; Pearl, 2009; Arjas, 2012). In predictive causal inference the parameters of the model are inferred with the available data so far and predictions made considering alternative scenarios.

To illustrate this lets first introduce a short notation  $\mathbf{y}_{\mathcal{J}_1,*} = \mathbf{y}_{\mathcal{J}_1}(\mathbf{x}_*, \mathbf{s}_*)$  and  $\mathbf{f}_{\mathcal{J}_1,*} = \mathbf{f}_{\mathcal{J}_1}(\mathbf{x}_*, \mathbf{s}_*)$  where  $\mathcal{J}_1$  denotes the set of species to be predicted and  $\mathcal{J}_2$  the *scenario species* assumed to be “managed”. For brevity, we omit the conditioning on hyperparameters. Then from the hierarchical structure of the model the conditional distribution of  $\mathbf{Y}_{\mathcal{J}_1}(\mathbf{x}_*, \mathbf{s}_*) | \mathbf{y}_{\mathcal{J}_2}$  can be written as

$$\pi(\mathbf{y}_{\mathcal{J}_1,*} | \mathbf{y}_{\mathcal{J}_2}) = \int \pi(\mathbf{y}_{\mathcal{J}_1,*} | \mathbf{y}_{\mathcal{J}_2}, \mathbf{f}_{\mathcal{J}_1,*}) \pi(\mathbf{y}_{\mathcal{J}_2}, \mathbf{f}_{\mathcal{J}_1,*}) d\mathbf{f}_{\mathcal{J}_1,*} / \pi(\mathbf{y}_{\mathcal{J}_2}) \quad (17)$$

where  $\mathbf{Y}_{\mathcal{J}_1}(\mathbf{x}_*, \mathbf{s}_*) | \mathbf{y}_{\mathcal{J}_2}, \mathbf{f}_{\mathcal{J}_1,*}$  only depends on  $\mathbf{f}_{\mathcal{J}_1,*}$ . This conditional predictive distribution can again be approximated with the Laplace approximation as shown in 7.3.

#### 4.2. Parameter inference

We used Laplace approximation (Rasmussen & Williams, 2006; Vanhatalo et al., 2010; Golding & Purse, 2016) to approximate the conditional posterior of latent variables  $\pi(\mathbf{f}_* | \mathbf{y}, \boldsymbol{\eta}, \Lambda)$  and the marginal likelihood of the hyperparameters  $\pi(\mathbf{y} | \boldsymbol{\eta}, \Lambda) = \int \pi(\mathbf{y} | \mathbf{f}, \boldsymbol{\eta}) \pi(\mathbf{f} | \Lambda) d\mathbf{f}$ . We searched for the (approximate) maximum a posterior (MAP) estimate for hyperparameters given by

$$(\hat{\boldsymbol{\eta}}, \hat{\Lambda}) = \arg \max_{\boldsymbol{\eta}, \Lambda} \log q(\mathbf{y} | \boldsymbol{\eta}, \Lambda) + \log \pi(\boldsymbol{\eta}, \Lambda). \quad (18)$$

where  $\log q(\mathbf{y} | \boldsymbol{\eta}, \Lambda)$  is the Laplace approximation for the log marginal likelihood for parameters. This approach is shown to produce good approximation for the posterior (predictive) distribution for latent variables (Vanhatalo et al., 2010; Golding & Purse, 2016), which are the main interest in this work. Hence, we fixed hyperparameters to their MAP estimate.

In order to avoid constrained optimization, all the parameters were transferred to unconstrained space. We used log transformation for covariance function parameters, and for the interspecific correlation matrices we used the transformation presented by Kurowicka & Cooke (2003) and Lewandowski et al. (2009), which is a bijective mapping between the space of correlation matrices and  $\mathbb{R}^{\binom{J}{2}}$ . This is summarized in 7.3. We used scaled conjugate gradient optimization for locating the MAP and checked carefully that a (local) mode had really been found by verifying that gradients along all hyperparameters were zero. The required gradients of  $\log q(\mathbf{y} | \boldsymbol{\eta}, \Lambda)$  were solved analytically as described by Rasmussen & Williams (2006) and Vanhatalo et al. (2010). The 7.3 summarizes the derivatives w.r.t. to the covariance parameters in  $\Sigma_\epsilon$ ,  $\Sigma_{h_r}$ ,  $r = 1, \dots, c$ . We implemented the models and computational methods to the GPstuff package (Vanhatalo et al., 2013).

## 5. Experiments

In this section we first illustrate the properties of the hierarchical multivariate GPs models with two simple examples. These examples are done in order to highlight particular properties of the proposed model. After this we introduce the model and analysis for the case study data (Section 2).

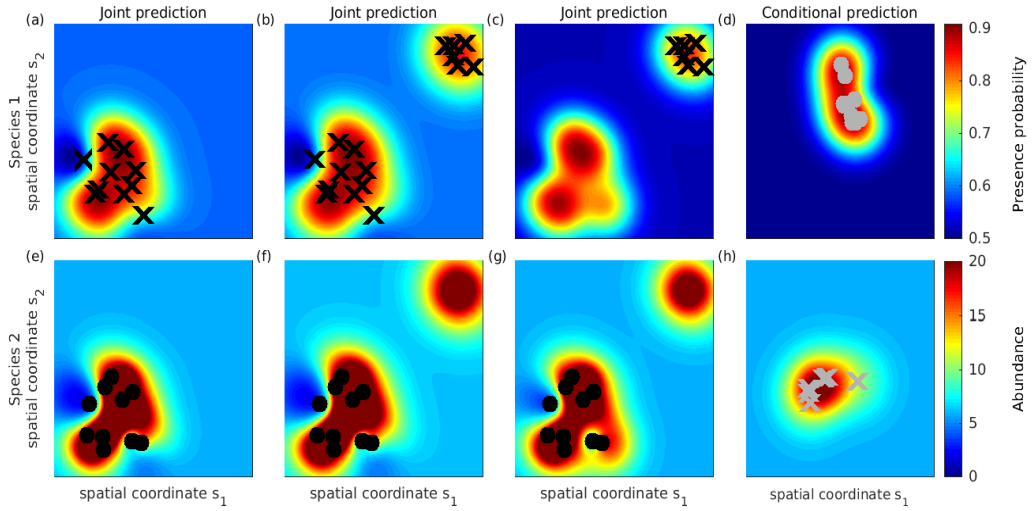


**Fig. 2.** Illustration of spatial multivariate GP prior for JSMD with two species and spatial only component. Crosses and dots are simulated data locations of species 1 (Binomial data) and species 2 (Negative-Binomial data). See text for discussion.

### 5.1. Demonstration with simulated spatial data

Figure 2 presents alternative simulated data and posterior predictions for spatial modelling of two species. The model follows spatial LMC; that is model (9), where the covariate terms are dropped out. The spatial correlation function used in this demo is the exponentiated square (Gaussian)  $k(\mathbf{s}, \mathbf{s}') = e^{-\|\mathbf{s} - \mathbf{s}'\|^2/2l^2}$ , where  $\|\mathbf{s} - \mathbf{s}'\|$  is the Euclidean distance and  $l$  is the length-scale. The first row of subplots shows the posterior predictive probability of observing species 1 ( $E[Y_1]$ ,  $Y_1(\mathbf{s}) \sim \text{Binomial}$ ) and the second row shows the expected number of species 2 ( $E[Y_2]$ ,  $Y_2(\mathbf{s}) \sim \text{Negative-Binomial}$ ). Plots (a) and (e) show the predictions when the species observations are from the same region but not from exactly the same locations. In this case the prediction of multivariate GP is similar to predictions by univariate GPs. Plots (b) and (f) show the predictions when data are available on both species from the lower left corner and additionally data on species 1 is available from upper right corner. There is positive correlation between species, which has been inferred from the data in the lower left region. Hence, the prediction for species 2 in upper right corner is informed by data on species 1 in that region. The last two columns illustrate the conditional scenario predictions (Section 4.1.4). In the third column the model has been trained with the data from the first column and the expected values in panels (c) and (g) show joint scenario prediction for both species assuming species in the new region were observed as shown in the panels. The fourth column is otherwise the same as the third column but now the conditional scenario prediction is done for both of the species separately.

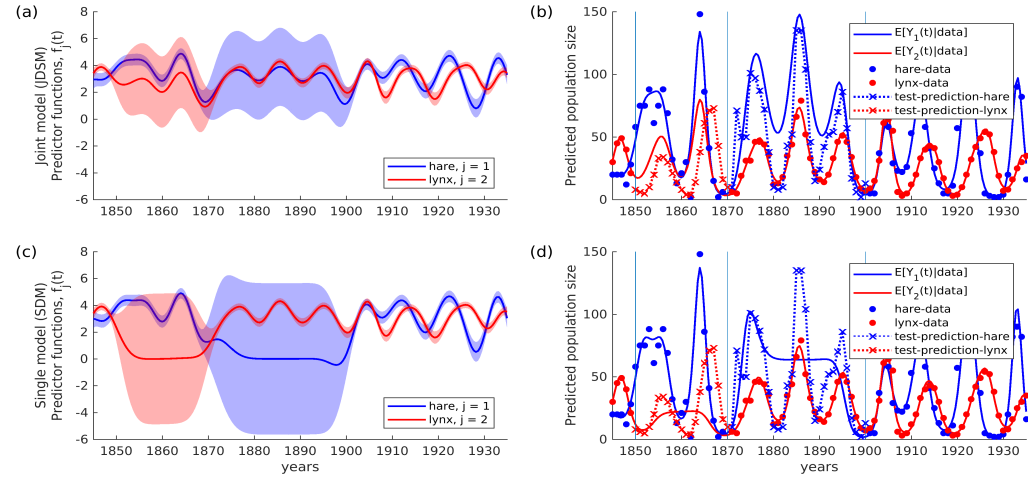


**Fig. 3.** The results from the analysis of hare and lynx interaction (predator-prey system) analyzed with single and joint SDM. Plots a) and c) show the posterior mean and 95% credible interval of the latent functions and plots b) and d) show the training data, test data and posterior expectation of observations. See text for explanation.

### 5.2. Demonstration with time series of species abundances

In this section we consider a classical predator-prey dataset containing the annual population count of hare and lynx in the north Canada through the period of 1845 to 1935 (Odum, 1953). The data is not spatially explicit since the observations are total counts over the north Canada, but it forms a time series for the population sizes. Hence, this analysis illustrates the behavior of individual additive covariate effect in the multivariate GP model (10) with time being the covariate. Let's denote by  $Y_{1,t}$  and  $Y_{2,t}$  the population sizes of hare and lynx at time  $t$ , and assume that  $Y_{1,t}|f_1(t) \sim \text{Poisson}(\exp(f_1(t)))$  and  $Y_{2,t}|f_2(t) \sim \text{Poisson}(\exp(f_2(t)))$ . We compared two alternative priors for the latent functions, one with independent GP priors and another with joint bivariate GP prior with the LMC structure. In order to compare models' predictive performances when some species have not been observed, we removed parts of the original data from the training set, the period of 1870-1900 for hare and 1850-1870 for lynx. Figure 3 displays the result of the data analysis. The model with bivariate GP prior clearly outperforms the independent model since it predicts better the test data points in periods where training data was removed. Moreover, its predictions have also smaller uncertainty than the predictions of independent GPs in those periods of time.

### 5.3. The case study on coastal species distribution

#### 5.3.1. Case study models

In our case study, none of the species observations correspond strictly to point location but since the area covered by sampling (photographs or fishing transect) is smaller than the resolution of environmental covariates and small compared to *a priori* expected

length-scale of spatial random effect we treat them as point observations. The vegetation and algae data are modeled with the Binomial model (3) and the fish data are modeled with the Negative-Binomial distribution (4). We compared the univariate additive GP (5), the LMC with additive independent predictor functions (9) and the multivariate additive GP (10). In each of these models, the spatial random effects were given the Matern covariance function with  $\nu = 3/2$  degrees of freedom  $k_{\epsilon_j}(\mathbf{s}, \mathbf{s}'; \sigma_j^2, \boldsymbol{\ell}_j) = \sigma_j^2 (1 + \sqrt{3} r_j(\mathbf{s}, \mathbf{s}')) \exp(-\sqrt{3} r_j(\mathbf{s}, \mathbf{s}'))$  where  $\sigma_j^2$  is the variance of the spatial process,  $\boldsymbol{\ell}_j^T = [\ell_{j,1} \ \ell_{j,2}]$  is the vector of length-scales and  $r_j(\mathbf{s}, \mathbf{s}') = [(\mathbf{s} - \mathbf{s}')^T (\text{diag}(\boldsymbol{\ell}_j)^2)^{-1} (\mathbf{s} - \mathbf{s}')]^{1/2}$ . The continuous covariate effects were given the exponentiated square covariance function. For the categorical covariate (Bottom class, table 1) we used a delta covariance function  $k_{h_{j,r}}(x_r, x'_r; \boldsymbol{\theta}) = \sigma_{\delta_j}^2 \delta_{x_r}(x'_r)$ , where  $\delta_{x_r}(x'_r) = 1$  if  $x_r = x'_r$  and zero otherwise. This corresponds to having an own intercept for each category. We used the marginally uniform priors (section 4.1.3) for the between species correlations and weakly informative priors for rest of the parameters. The variance parameters were given Student- $t(\mu = 0, \sigma^2 = 4, \nu = 4)$  priors and the length-scale parameters were given Inverse-Student- $t(\mu = 0, \sigma^2 = 1, \nu = 4)$ . Hence, *a priori* more weight is given for smooth functions with small variability.

### 5.3.2. Model validation

Our aim is to provide models that give reliable posterior predictions. Hence, it is natural to compare the different models with the goodness of their posterior predictive distributions. This can be done efficiently with cross validation using the log predictive density diagnostics (Vehtari & Ojanen, 2012). Let  $\mathcal{D}$  denote the full data-set. Fix  $K$  disjoint sub-sets of  $\mathcal{D}$ , say  $\mathcal{D}_1, \dots, \mathcal{D}_K$ , such that their union is  $\mathcal{D}$ . The  $K$ -fold cross-validation log point-wise marginal predictive density is then  $L_K(\mathcal{D}) = \frac{1}{n} \sum_{i=1}^n \log \pi(y_i | \mathcal{D}_{\sim k(i)})$  where  $\mathcal{D}_{\sim k(i)} = \{\cup_{r=1}^K \mathcal{D}_r : r \neq k(i)\}$  and  $k(i)$  is such that  $y_i \in \mathcal{D}_{k(i)}$ . Here, we compare the models with the leave-one-out cross-validation (LOO-CV,  $K = n$ ) and structured 5-fold cross-validation. In both comparisons we used the MAP estimate for the hyperparameters. Since our data set is rather large, leaving only one data point out of the training set has only negligible effect on the posterior of the hyperparameters. Hence, the LOO-CV was conducted at the MAP found with full data. Moreover, we used EP to approximate the LOO-CV log predictive densities (Vanhatalo et al., 2013). The 5-fold cross-validation was conducted by finding the MAP of each training set.

The rationale of calculating both LOO-CV and 5-fold CV comparison is the following. Since multiple species were sampled at every sampling site and each of the sampling sites has other sites spatially nearby it, the LOO-CV log predictive densities are affected significantly by the spatial random effects. Hence, the LOO-CV measures models' interpolation performance which can be good even if the models were not able to infer well the response along covariates (predictor functions) (Vanhatalo et al., 2012; Veneranta et al., 2013). For this reason, we structured the 5-fold cross-validation by dividing the data into five spatially distinct groups corresponding to regions I-V in Figure 1. The sampling sites in different groups are spatially so far from each others that the spatial random effects do not affect the posterior predictive distributions for test group practically at all. Hence, the 5-fold cross-validation tests mostly the extrapolation performance of a

**Table 2.** Model comparison with leave-one-out (LOO) and 5-fold cross validation using the mean point wise log marginal predictive density statistics (and its standard error). The bolded numbers show the overall performance over all species and the indented text shows the species specific predictions.

GP models	LOO Cross Validation	5-fold Cross validation
<b>Univariate add. (5)</b>	<b>-2.230 (0.082)</b>	<b>-2.465 (0.094)</b>
diatom.algae	-3.942 (0.225)	-4.002 (0.225)
filame.algae	-4.568 (0.141)	-4.692 (0.146)
macro-veg	-1.909 (0.234)	-2.092 (0.240)
threespine-sb	-1.477 (0.157)	-1.624 (0.154)
ninespine-sb	-1.334 (0.151)	-1.464 (0.149)
white-fish	-2.840 (0.200)	-3.092 (0.216)
vendace	-1.634 (0.210)	-2.196 (0.314)
<b>Add. ind. predictors (9)</b>	<b>-2.081 (0.080)</b>	<b>-2.480 (0.100)</b>
diatom.algae	-3.578 (0.232)	-4.010 (0.217)
filame.algae	-4.104 (0.159)	-4.680 (0.135)
macro-veg	-1.733 (0.223)	-2.148 (0.252)
threespine-sb	-1.385 (0.149)	-1.637 (0.156)
ninespine-sb	-1.232 (0.139)	-1.489 (0.151)
white-fish	-2.782 (0.203)	-3.092 (0.213)
vendace	-1.537 (0.204)	-2.215 (0.316)
<b>Add. mult. predictors (10)</b>	<b>-1.669 (0.080)</b>	<b>-2.316 (0.086)</b>
diatom.algae	-2.307 (0.112)	-3.947 (0.217)
filame.algae	-1.244 (0.751)	-4.623 (0.140)
macro-veg	-1.289 (0.150)	-1.950 (0.248)
threespine-sb	-1.210 (0.140)	-1.509 (0.156)
ninespine-sb	-1.184 (0.147)	-1.389 (0.149)
white-fish	-3.399 (0.393)	-2.964 (0.205)
vendace	-2.041 (0.451)	-1.837 (0.247)

model, which is governed by the goodness of the predictor functions, whereas the LOO-CV tests the interpolation performance, which is governed also by the spatial random effects.

## 6. Results

### 6.1. Predictive performance of models

Table 2 summarizes the cross-validation comparisons. The additive multivariate predictors model (10) is clearly the best in both LOO and 5-fold cross validation. It has the best overall performance over all species and performs best in extrapolation (5-fold cross validation) for each species individually. However, it is the worst in the interpolation (leave-one-out cross validation) of whitefish and vendace in which case the additive independent predictors model (9) works best. The additive independent predictors model works better than the univariate additive model in interpolation (LOO-CV) for all species individually and jointly. However, these models are in practice equally good in extrapolation (5-fold CV). Hence, multivariate spatial random effect improved interpolation whereas multivariate predictors improved the extrapolation.

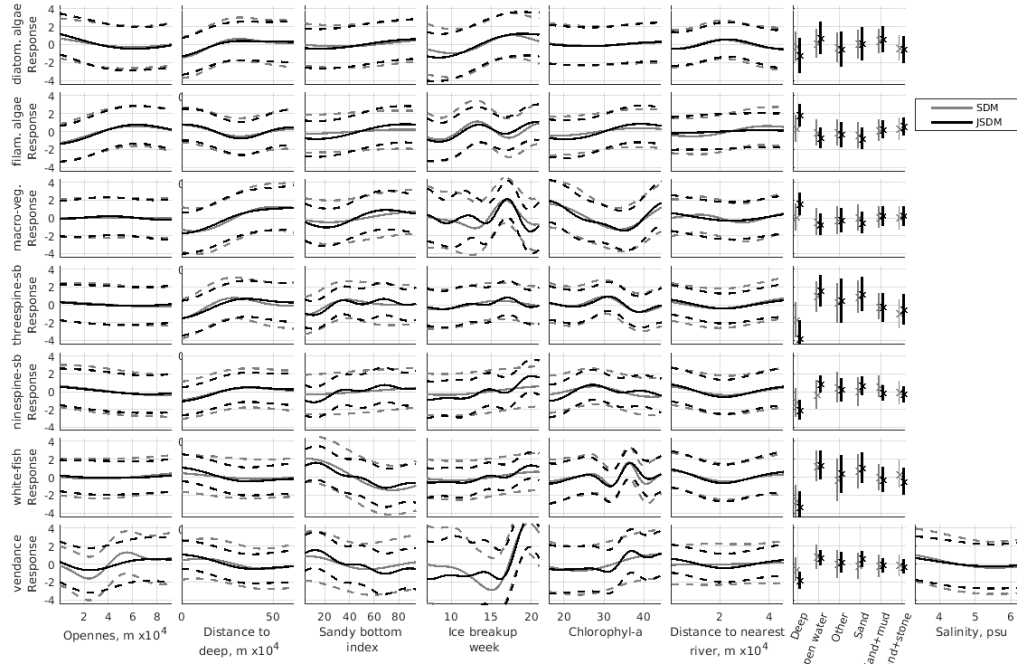


**Fig. 4.** Marginal latent responses along covariates,  $h_{j,r}$ . Grey corresponds to single species model and black to multivariate additive GP model.

## 6.2. Effects of environmental covariates

Figure 4 shows the marginal effect of the predictor functions for both SSDM and JSDM models calculated as detailed in section 4.1.2. In general, the responses in JSDM and SSDM are similar. In most of the cases the uncertainty in response function is smaller (narrower credible regions) in JSDM than in SSDM although the differences are not large. Most of the responses are very smooth and such that they could easily be fitted also with traditional linear or quadratic models. However, in case of, for example, three and nine spine stickleback, macrovegetation and filamentous algae either distance to deep or openness show logistic style response where the increasing/decreasing response levels off. Moreover, the response of vendace on ice break up week is first constant but has very steep increase after week 16. The responses to ice break up or chlorophyl-a show non-linear and non-quadratic responses also for white fish, macrovegetation and filamentous algae.

The interspecific correlations (Figure 5) show that the responses to environment are, in general, similar among Coregonids and among sticklebacks whereas there are clear differences among these groups. These fish groups respond differently to sandy bottom and distance to deep. Moreover, there is strong positive spatial correlation among Coregonids and among sticklebacks but not between these groups. All species have negative spatial correlation with filamentous algae whereas there is either weak positive or negligible spatial correlation between fish species and macrovegetation and

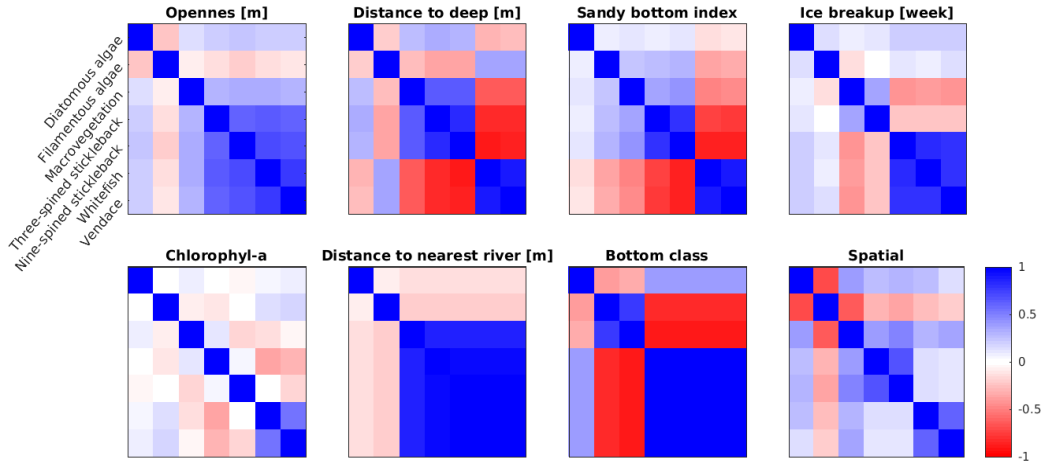


**Fig. 5.** The maximum a posterior estimate of the correlation matrices in the multivariate additive GP model with squared-exponential covariance function.

diatomous algae. The MAP of other parameters is summarized in 7.3.

### 6.3. Spatial predictions

Figure 6 shows the distribution maps as posterior median of intensity and expected count of individuals in replicate sampling produced by SSDM and JSDM for vendace. The distribution maps for other species are shown in 7.3. The posterior median is a direct function of the posterior mean of the latent function whereas the expected counts depend also on the posterior uncertainty so that the expectation is the larger the larger the uncertainty (see 7.3). In broad scale the posterior median of the intensity look similar with SSDM and JSDM whereas SSDM predicts larger species counts than JSDM for all species throughout the study region. Hence, the uncertainty related to SSDM predictions is larger than that of JSDM predictions. Both SSDM and JSDM predict that vendace is distributed mostly in the northern Gulf of Bothnia. However, SSDM predicts somewhat higher median intensity than JSDM also in the southern Gulf of Bothnia. In relation to median intensity similar pattern that JSDM predicts more restricted distribution range than the single species model is seen also in the predictions concerning sticklebacks and whitefish. In case of diatomous and filamentous algae SSDM and JSDM predict the distribution pattern similarly whereas for macrovegetation JSDM predicts slightly larger distribution ranges. The posterior distributions of spatial lenght-scale parameters were concentrated near one kilometer or less (see 7.3) for which reason the differences in distribution predictions cannot be explained by the spatial random effects over large areas but the spatial random effect explains local deviations from the predictions based on covariates.

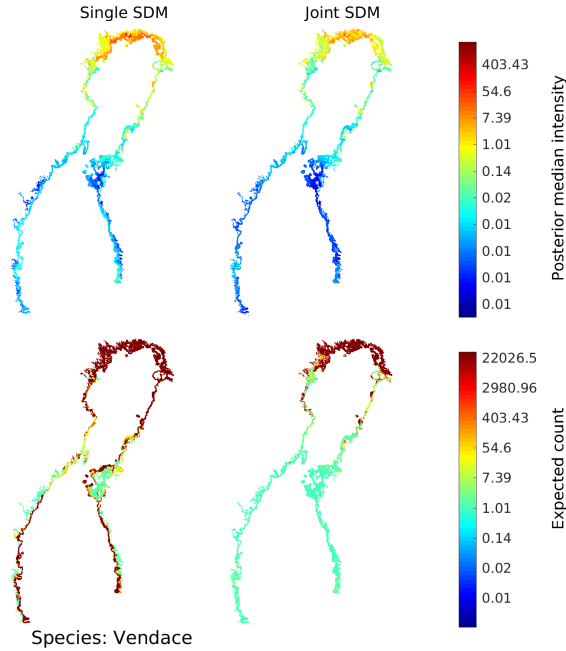


**Fig. 6.** Posterior predictive median of intensity and the expected count of individuals in replicate sampling for vendace.

## 7. Discussion and concluding remarks

### 7.1. Case study results

In general JSDM had better predictive performance than the independent single species models. The qualitative differences between the results from these models are most apparent in the distribution maps and predictor functions. The JSDM predicted in general smaller distribution ranges than the single species models (macrovegetation being only exception to this general pattern) and the posterior uncertainty in their predictions were smaller than in single species models.

When interpreting the results, it should be remembered that the sampling was targeted to larvae of sea-spawning Coregonids (whitefish and vendace) and planned to cover their plausible distribution range in terms of spatial (coastal areas of Gulf of Bothnia) and temporal extent (spring). Other species were sampled alongside Coregonids and the sampling area covers only limited portion of their full distribution range in the spring. Moreover, the abundance and distribution of all the studied species varies annually. Fish change their distribution areas seasonally and their larval stages last only few weeks. Vegetation and algal cover vary due changes in temperature and ice effects. For these reasons the results are most representative for larvae of whitefish and vendace and for other species describe their distribution in the shallow coastal regions only.

The results correspond rather well to earlier knowledge on the studied species. The responses to environmental covariates and interspecific correlations (Figures 4 and 5) indicate that whitefish and vendace larvae are, in general, distributed in different areas than sticklebacks. Most of the literature on sticklebacks in the Baltic Sea focuses on three spined sticklebacks whereas nine spined stickleback is not well studied. In early spring, the stickleback abundances have been found to be highest in sheltered archipelago areas, where part of the population overwinter. High abundance of sticklebacks are typically thought to indicate structural complexity on the bottom; such as presence of stones and boulders as well as reeds or other macrovegetation that function as a shelter and provide also food items like grazers (Peltonen et al., 2004; Sieben et al., 2011). On contrary, highest densities of whitefish and vendace larvae are observed in open sandy shores, where the distance to deep areas is short and shores are structurally simple, without macrovegetation, boulders and stones (Hudd et al., 1988; Leskelä et al., 1991; Veneranta et al., 2013).

The distribution of vendace is highly influenced by ice break up week and salinity so that long ice cover period and low salinity increase the abundance. The length of ice winter is longer and salinity is lower in the northern than in the southern Gulf of Bothnia and thus it correlates positively to Coregonid presence (Vanhatalo et al., 2012). In general, optimal habitats for Coregonid larvae are mainly located in the northernmost Gulf of Bothnia which is seen also in the distribution maps of vendace and whitefish.

Sticklebacks are known to prey mainly on mesozooplankton, but also on grazers (Peltonen et al., 2004; Sieben et al., 2011). Sticklebacks feed also on fish larvae if available (Byström et al., 2015), but there are no studies on potential predation risk to Coregonids. Based on our results, in the scale of coastal region of Gulf of Bothnia, sticklebacks are not threat to Coregonid larvae since their distribution areas do not overlap with areas where Coregonid density is high. Moreover, there was no spatial correlation between sticklebacks and coregonids (Figure 5) which could indicate interspecific interaction of any kind. The presence of sticklebacks has been connected to the higher eutrophication status and stickleback reproduction and growth benefit from increasing temperature and eutrophication (Lefébure et al., 2011; Candolin et al., 2008; Meier et al., 2012) On contrary, these environmental characteristics are assumed to reflect negatively the Coregonid reproduction success (M.Cingi et al., 2010; Müller, 1992; Veneranta et al., 2013; Vanhatalo et al., 2012). In our results whitefish and vendace larvae have positive response on Chlorophyl-a, which is a strong indicator for increasing eutrophication. However, Chlorophyl-a concentration is typically higher also near river mouths where salinity is lower and nutrient inflow from drainage areas high. Hence the result more likely reflects the high river influence through low salinity than preference for eutrophicated water.

Since we are examining early spring distribution the vegetation and algae distribution reflect the nutrient status during winter and early spring as well as effect of ice cover and ice scraping in wind exposed shallow areas. Both the SSDM and JSDM indicate that filamentous algae occur in all coastal areas in high densities, except some sheltered inner coastal areas. Macrovegetation and diatomous algae had highest presence probabilities at areas with lower filament presence probability. This pattern is well in line with the general understanding of these species groups. Filamentous algae are typically distributed in wind and wave exposed shores, that epiphytic diatoms and reeds that require

shelter cannot tolerate. However, filamentous algae can also grow over macrovegetation and it is possible that macrovegetation distribution is underestimated since at some areas filamentous algae growth over macrovegetation might have hidden macrovegetation from the sampling pictures. In earlier studies, the higher nutrient levels in sheltered areas have been found to affect positively on reed belt growth, and especially high abundance of macrovegetation species have been found from archipelago areas, lagoons and bays as well as in river inlets (Pitkänen et al., 2013; Altartouri et al., 2014; Meriste & Kirsimae, 2015). The JSDM model reflects these smaller scale occurrences better than SSDM and fits better to the distribution pattern. Diatomous algae are more common in estuaries and northern parts of the study area (see 7.3) which in our model is likely explained by longer ice winter towards northern Gulf of Bothnia and distance to deep water. However, these covariates correlate strongly with salinity which Snoeijs (1995) found to be the overriding environmental factor regulating the distribution of epiphytic diatoms in the Baltic Sea level.

## 7.2. Multivariate additive Gaussian process

The key idea in most of the JSDMs is to add interspecific correlations (or other dependencies) in the model structure. In that respect, the proposed multivariate additive Gaussian process model (10) is closely related to existing JSDMs. However, all the existing models are based on generalized linear modeling framework for which reason the multivariate additive Gaussian process model makes an important contribution by extending JSDMs to semiparametric models. Next we discuss in more detail some of the most important links and differences to existing models, with special emphasis on relation to the recently published hierarchical model of species communities (HMSC) framework Ovaskainen et al. (2017), and highlight the novel methodological contributions in this paper.

### 7.2.1. Interspecific correlations

From the predictive point of view, the interspecific correlations in predictive functions are attractive for many reasons. In many applications of SDMs the aim is to predict species distribution over regions that include locations spatially far from the data (Record et al., 2013) or to conduct scenario predictions related to, for example, climate change or land use (Guisan et al., 2013; Angelieri et al., 2016). In these applications, predictions are based on the inferred predictive functions of environmental covariates. The inclusion of interspecific dependence allows information flow between species which improves the estimates for predictive functions especially for species with only scarce data (Ovaskainen & Soininen, 2011; Ovaskainen et al., 2017; Hui et al., 2013; Clark et al., 2014).

We used the marginally uniform priors of Barnard et al. (2000) and Tokuda et al. (2012) for the interspecific correlations between predictor functions and spatial random effects. This is justified by prior ignorance on correlations but we could have chosen other priors as well. Prior information on interspecific correlations could be incorporated into model with, e.g., informative inverse Wishart prior. As the number of species increases it becomes increasingly hard to infer the full covariance matrix in which case we could follow Ovaskainen et al. (2016b) who proposed to use spatially

dependent latent factors which induce for the spatial random effects a covariance structure  $\text{Cov}(\epsilon_j(\mathbf{s}), \epsilon'_j(\mathbf{s}')) = \sum_{q=1}^M \lambda_{qj} \lambda_{qj'} k_q(\mathbf{s}, \mathbf{s}')$ , where  $k_q$  is the  $q$ 'th spatial covariance function and  $\lambda_{qj}$  the corresponding species specific factor loading. Here,  $M < J$  so that this covariance structure is a low rank representation of LMC (Anderson & Rubin, 1956; Lopez, 2000; Lopez et al., 2008). Latent factor representation was considered also by Taylor-Rodríguez et al. (2016) who propose a clustering scheme where the species are clustered to less than  $J$  factor loading vectors.

The correlation structure between response functions has received less interest in the literature and most often the response functions are treated mutually independent among species. Important exception are species archetype models (Dunstan et al., 2013) and the HMSC framework of Ovaskainen et al. (2017). In the latter, the response functions are defined as  $h_j(\mathbf{x}_j) = \mathbf{x}_j \theta_j$ , where  $\theta = [\theta_1^T, \dots, \theta_J^T]^T$  is a  $J \times p$  matrix of regression weights with hierarchical prior. In HMSC species specific weights are given a Gaussian prior  $\theta_j \sim N(\mu_j, V_j)$  where  $\mu_j$  is the species specific mean that can be common for all species, common within groups of species or modelled through species traits  $\mu_{jr} = \tau_j^T \gamma_r$  where  $\tau_j$  is a vector of traits of species  $j$  and  $\gamma_r \sim N(0, V_\gamma)$  are the effects of traits to response along covariate  $r$ . With  $V = \sigma^2 I_{J \times J}$  and common prior mean  $\mu_j = \mu \sim N(0, \sigma_\mu^2)$  for all  $j \in 1, \dots, J$ , the induced covariance between species specific additive response functions is

$$\begin{aligned} \text{Cov}(h_{j,r}(x_r), h_{j',r}(x'_r)) &= \mathbb{E}[\text{Cov}(x_r \theta_{jr}, x'_r \theta_{j'r})] + \text{Cov}(\mathbb{E}[x_r \theta_{jr}], \mathbb{E}[x'_r \theta_{j'r}]) \\ &= (\sigma_\mu^2 + \delta_j(j')\sigma^2)x_r x'_r \end{aligned}$$

and with trait dependent prior mean  $\text{Cov}(h_{j,r}(x_r), h_{j',r}(x'_r)) = (\tau_j^T V_\gamma \tau_{j'} + \delta_j(j')\sigma^2)x_r x'_r$ . Hence, these alternatives can be seen as additive multivariate GPs (10) with covariance functions  $k_{h_{j,r}} = x_r x'_r$ , for all  $j = 1, \dots, J$ , and interspecific covariances  $\Sigma_{h_r} = \sigma_\mu^2 + \delta_j(j')\sigma^2$  and  $\Sigma_{h_r} = \tau_j^T V_\gamma \tau_{j'} + \delta_j(j')\sigma^2$ . Hence, the HMSC could easily be extended to semiparametric models as well. These hierarchical model structures of Ovaskainen et al. (2017) contain prior information with realistic ecological interpretation and, hence, using the induced interspecific covariance structure in the additive multivariate GP model would make it ecologically more realistic and potentially improve its predictive performance. The HMSC framework has many other features as well, such as the inclusion of phylogenetic relationships, which could in principle be incorporated in our approach as well. The structure of interspecific correlations is likely to be especially important in scenario based predictive analyses, such as climate change predictions.

### 7.2.2. On response functions

The regression function in species distribution models is of central importance, providing basis to understand which factors affect species distribution pattern, how they are affected, and to predict the species distribution in new areas. Linear and other parametric models are efficient in finding the overall trends in responses but have trouble in locating abrupt changes in response function and change points in abundance due, for example, physical tolerance limits. Such limits, for example, along temperature and salinity are typical for large variety of taxa in aquatic domains (Pauly, 1980; Boeuf & Payan, 2001; MacKenzie et al., 2007) and, for example, Vanhatalo et al. (2012), Shelton

et al. (2014), Golding & Purse (2016) and Kallasvuo et al. (2017) have demonstrated the benefits from using semiparametric models in single species case. The GP approach for modeling environmental responses is similar to generalized additive models (Guisan et al., 2002). However, the latter models have not been implemented as JSDMs. A clear disadvantage from using semiparametric models compared to more restricted parametric models is that inferring the responses reliably requires typically more data or more prior information to restrict the implausible responses (Golding & Purse, 2016). The multivariate additive GP helps in this problem as well since the interspecific correlations effectively increase the amount of data to be used to infer each response function and hence decreases the uncertainty related to them.

Even though multivariate additive GP framework allows generic model description it opens also several new questions related to the choice of covariance functions and interspecific correlations. A typical choice for general purpose covariance function is the exponentiated square or other radial basis function. However, predictions using these covariance functions revert to prior predictive distributions when predicting beyond covariate range covered by data. Hence, in extrapolation tasks stationary covariance functions may not be the optimal choice (Vanhatalo et al., 2012; Kallasvuo et al., 2017). Hence, we would anticipate that combining the multivariate GP models with functional constraints, such as monotonicity information (Riihimäki & Vehtari, 2010) or saturating behaviour Honkela et al. (2015), could improve models predictive performance.

#### 7.2.3. Spatial random effects

It has been demonstrated in many other earlier works that current environmental conditions alone may not sufficiently explain species distribution and spatial random effects improve their predictive performance (Latimer et al., 2006; Vanhatalo et al., 2012; Clark et al., 2014; Kallasvuo et al., 2017). This is reasonable, since the distribution of species is shaped by the interplay of environmental covariates, stochastic processes and species interaction (Ovaskainen et al., 2017). Hence, a justified model should account for random processes and as demonstrated also by our results also to species interactions in these processes.

#### 7.2.4. Posterior inference and predictive properties

The JSDM built with multivariate additive GP had clearly the best overall predictive performance. Moreover, the uncertainty in the predictions by JSDM were smaller than in the SSDMs and, hence, the predictions can be concluded to be more accurate. These findings have important implications to practical use of SDMs for management and other purposes. For example Kallasvuo et al. (2017) used SSDMs to classify coastal areas of Finland to unsuitable, suitable and highly productive spawning regions for four commercially important fish species. They based their estimates on the differences in expected numbers of larvae between areas which, as shown by Figure 6 is highly sensitive to the uncertainty of the predictions. Moreover, by using SSDMs we can overestimate the total biomass of all species (Clark et al., 2014).

However, an evident challenge with multivariate additive GP is the computation related to hyperparameter and latent variable inference. The core elements in the multi-

variate additive GP is the covariance matrix induced by the GP components. With many species and sampling sites the covariance matrix increases fast making the implementation easily infeasible. Here we used Laplace method to speed up the computation by decreasing the number of costly posterior density calculations compared to full MCMC. However, in order to scale up the methods for large data sets, the model would need to be implemented more efficiently so that we do not need to store and invert full  $nJ \times nJ$  matrices. One option to reduce the computational time could be to exploit the property that linear LMC can be parameterized through species specific conditional distributions (Gelfand et al., 2004). Another option could be to implement multivariate GPs with sparse GP approximations (Vanhatalo et al., 2010; Alvarez et al., 2010; Alvarez & Lawrence., 2011). However, we leave these considerations for future.

### 7.3. Summary

Our multivariate additive GP based JSDM combines the key ideas from semiparametric SSDMs and state-of-the-art parametric JSDMs. It shows superior performance compared to analogous SSDMs and can improve analysis and predictions compared to existing JSDMs. The core model structure of the state-of-the-art joint species distribution modeling framework HMSC (Ovaskainen et al., 2017) is similar to our additive multivariate GP. Hence, the multivariate additive GP can be seen as the first step towards integration of the semiparametric SSDMs presented by Vanhatalo et al. (2012) and Golding & Purse (2016) and hierarchical JSDMs of Ovaskainen et al. (2017). Moreover, the methods presented here are not restricted only to species distribution modelling but can be used in wide variety of other applications as well.

### Supplementary material

The supplementary material contains additional mathematical formulation of the methodology proposed in this paper and additional figures and tables for the case study analysis.

### Acknowledgements

This work has bee funded by the Academy of Finland (grant 304531) and Research Funds of the University of Helsinki (decision No. 465/51/2014).

### References

- Altartouri, A., Nurminen, L., & Jolma, A. (2014). Modeling the role of the close-range effect and environmental variables in the occurrence and spread of *phragmites australis* in four sites on the finnish coast of the gulf of finland and the archipelago sea. *Ecology and Evolution*, 4, 987–1005.
- Alvarez, M. A., & Lawrence., N. D. (2011). Computationally efficient convolved multiple output Gaussian processes. *Journal of Machine Learning Research*, 12, 1425–1466.

- Alvarez, M. A., Luengo, D., Titsias, M. K., & Lawrence., N. D. (2010). Efficient multi-output Gaussian processes through variational inducing kernels. *JMLR Workshop and conference proceedings*, 9, 25–32.
- Anderson, T. W., & Rubin, H. (1956). Statistical inference in factor analysis. In *Proceedings of the Third Berkeley Symposium on Mathematical Statistics and Probability*, vol. V. University of California, Berkeley, Third Berkely Symposium on Mathematical Statistics and Probability.
- Angelieri, C. C. S., Adams-Hosking, C., Ferraz, K. M. P. M. d. B., de Souza, M. P., & McAlpine, C. A. (2016). Using species distribution models to predict potential landscape restoration effects on puma conservation. *PLOS ONE*, 11(1), 1–18.
- Arjas, E. (2012). Causal inference from observational data: a Bayesian predictive approach. In C. Berzuini, P. Dawid, & L. Bernardinelli (Eds.) *Causality: Statistical Perspectives and Applications*, (pp. 71–83).
- Austin, M. (2007). Species distribution models and ecological theory: A critical assessment and some possible new approaches. *Ecological Modelling*, 200(1-2), 1–19.
- Banerjee, S., Carlin, B. P., & Gelfand, A. E. (2015). *Hierarchical Modelling and Analysis for Spatial Data*. Chapman Hall/CRC, second ed.
- Barnard, J., McCulloch, R., & Meng, X.-L. (2000). Modelling covariance matrices in terms of standard deviations and correlations, with applications to shrinkage. *Statistica Sinica*.
- Bergström, U., Olsson, J., Casini, M., Eriksson, B. K., Fredriksson, R., Wennhage, H., & Appelberg, M. (2015). Stickleback increase in the baltic sea – a thorny issue for coastal predatory fish. *Estuarine, Coastal and Shelf Science*, 163, 134–142.
- Bickel, P., & Doksum, K. A. (1977). *Mathematical Statistics: Basic Ideas and Selected Topics*. No. v.1 in Holden-Day Series in Probability and Statistics. Prentice Hall.
- Boeuf, G., & Payan, P. (2001). How should salinity influence fish growth? *Comparative Biochemistry and Physiology Part C: Toxicology & Pharmacology*, 130, 411–423.
- Borja, A., Elliot, M., Andersen, J., Cardoso, A., Cartensen, J., ao Ferreira, J., Heiskanen, A.-S., ao Marques, J., ao Neto, J., Teixeira, H., Uusitalo, L., Uyarra, M., & Zampoukas, N. (2003). Good environmental status of marine ecosystems: What is it and how do we know we have attained it? *Marine Pollution Bulletin*.
- Busse, S., & Snoeijs, P. (2002). Gradient responses of diatom communities in the bothnian bay, northern baltic sea. *Nova Hedwigia*, 3-4, 501–525.
- Byström, P., Bergström, U., Hjälten, A., Ståhl, S., Jonsson, D., & Olsson, J. (2015). Declining coastal piscivore populations in the baltic sea: Where and when do sticklebacks matter? *Ambio*, 44, 462–471.
- Candolin, U., EngströmÖst, J., & Salesto, T. (2008). Human-induced eutrophication enhances reproductive success through effects on parenting ability in sticklebacks. *Oikos*, 117, 459–465.

- Chib, S., & Greenberg, E. (1998). Analysis of multivariate probit models. *Biometrika*, 85(2), 347–361.
- Clark, J. S., Gelfand, A., Woodall, C. W., & Zhu, K. (2014). More than the sum of the parts: forest climate response from joint species distribution models. *Ecological Applications*, 24(5), 990–999.
- Cressie, N., & Wikle, C. K. (2011). *Statistics for Spatial-Temporal Data*. Wiley Series in Probability and Statistics.
- Dunstan, P. K., Foster, S. D., Hui, F. K. C., & Warton, D. I. (2013). Finite Mixture of Regression Modeling for High-Dimensional Count and Biomass Data in Ecology. *Journal of Agricultural, Biological, and Environmental Statistics*, 18(3), 357–375.
- Duvenaud, D., Nickisch, H., & Rasmussen, C. (2011). Additive gaussian processes. *Neural Information Processing Systems*.
- Elith, J., & Leathwick, J. R. (2009). Species distributions models: Ecological explanation and predictions across space and time. *The Annual Review of Ecology, Evolution and Systematics*, 40(677-697).
- Eriksson, B. K., Ljunggren, L., Sandstrom, A., Johansson, G., Mattila, J., Rubach, A. E., Råberg, S., & Snickars, M. (2009). Declines in predatory fish promote bloomforming macroalgae. *Ecological Applications*, 19, 1975e1988.
- Eriksson, B. K., Rubach, A., Batsleer, J., & Hillebrand, H. (2012). Cascading predator control interacts with productivity to determine the trophic level of biomass accumulation in a benthic food web. *Ecological Research*, 27, 203e210.
- Gelfand, A. E., Jr, J. A. S., Wu, S., Latimer, A., Lewis, P. O., Rebelo, A. G., & Holder, M. (2006). Explaining species distribution patterns through hierarchical modelling. *Bayesian Analysis*, 1(1), 41–92.
- Gelfand, A. E., Schmidt, A. M., Banerjee, S., & Sirmans, C. F. (2004). Nonstationary multivariate process modeling through spatially varying coregionalization. *Test*, 13(2), 263–312.
- Golding, N., & Purse, B. V. (2016). Fast and flexible bayesian species distribution modelling using gaussian processes. *Methods in Ecology and Evolution*, 7, 598–608.
- Guisan, A., Edwards, T. C., & Hastie, T. (2002). Generalized linear and generalized additive models in studies of species distributions: setting the scene. *Ecological Modelling*, 157(2-3), 89–100.
- Guisan, A., Tingley, R., Baumgartner, J. B., Naujokaitis-Lewis, I., Sutcliffe, P. R., Tulloch, A. I. T., Regan, T. J., Brotons, L., McDonald-Madden, E., Mantyka-Pringle, C., Martin, T. G., Rhodes, J. R., Maggini, R., Setterfield, S. A., Elith, J., Schwartz, M. W., Wintle, B. A., Broennimann, O., Austin, M., Ferrier, S., Kearney, M. R., Possingham, H. P., & Buckley, Y. M. (2013). Predicting species distributions for conservation decisions. *Ecology Letters*, 16(12), 1424–1435.

- Hartmann, M., Hosack, G. R., Hillary, R. M., & Vanhatalo, J. (2017). Gaussian process framework for temporal dependence and discrepancy functions in ricker-type population growth models. *Ann. Appl. Statist.*, 11(3), 1375–1402.
- Hastie, T., & Tibshirani, R. (1986). Generalize additive models. *Statistical Science*, 1(3), 297–318.
- Helsinki Comission (Ed.) (2009). *Biodiversity of the Baltic sea: An integrated thematic assessment on biodiversity and nature conservation in the Baltic sea*, 116B.
- Honkela, A., Peltonen, J., Topa, H., Charapitsa, I., Matarese, F., Grote, K., Stunnenberg, H. G., Reid, G., Lawrence, N. D., & Rattray, M. (2015). Genome-wide modeling of transcription kinetics reveals patterns of rna production delays. *Proceedings of the National Academy of Sciences*, 112(42), 13115–13120.  
URL <http://www.pnas.org/content/112/42/13115>
- Hudd, R., Lehtonen, H., & Kurttila, I. (1988). Growth and abundance of fry; factors which influence the year-class strength of whitefish (*Coregonus lavaretus widegreni*) in the southern bothnian bay (baltic). *Finnish Fisheries Research*, 9, 213–220.
- Hui, F. K. C., Warton, D. I., Foster, S. D., & Dunstan, P. K. (2013). To mix or not to mix: Comparing the predictive performance of mixture models vs. separate species distribution models. *Ecology*, 94(9), 1913–1919.
- Illian, J., Martino, S., Sørbye, S. H., Gallego Fernández, J. B., Zunzunegui, M., Esquivias, M. P., Travis, J. M. J., & Warton, D. (2013). Fitting complex ecological point process models with integrated nested Laplace approximation. *Methods in Ecology and Evolution*, 4(4), 305–315.
- Johnston, A., Fink, D., Reynolds, M. D., Hochachka, W. M., Sullivan, B. L., Bruns, N. E., Hallstein, E., Merrifield, M. S., Matsumoto, S., & Kelling, S. (2015). Abundance models improve spatial and temporal prioritization of conservation resources. *Ecological Applications*, 25(7), 1749–1756.
- Kallasvuo, M., Vanhatalo, J., & Veneranta, L. (2017). Modeling the spatial distribution of larval fish abundance provides essential information for management. *Canadian Journal of Fisheries and Aquatic Sciences*, 74, 636–649.
- Kurowicka, D., & Cooke, R. (2003). A parameterization of positive definite matrices in terms of partial correlation vines. *Linear Algebra and its Applications*, 372(Supplement C), 225–251.
- Latimer, A. M., Wu, S., Gelfand, A. E., & Silander, Jr., J. A. (2006). Building statistical models to analyze species distributions. *Ecological Applications*, 16(1), 33–50.
- Lefébure, R., Larsson, S., & Byström, P. (2011). A temperature dependent growth model for the threespined stickleback *Gasterosteus aculeatus*. *Journal of fish biology*, 79, 1815–1827.

- Leskelä, A., Hudd, R., Lehtonen, H., Huuhmarniemi, A., & Sandström, O. (1991). Habitats of whitefish (*Coregonus lavaretus* (L.) s.l.) larvae in the gulf of bothnia. *Aqua Fennica*, 21, 145–151.
- Lewandowski, D., Kurowicka, D., & Joe, H. (2009). Generating random correlation matrices based on vines and extended onion method. *Journal of Multivariate Analysis*, 100(9), 1989–2001.
- Lindley, D. V. (2002). Seeing and Doing: The Concept of Causation. *International Statistical Review*, 70(2), 191–214.
- Lopez, H. F. (2000). *Bayesian Analysis in Latent Factor and Longitudinal Models*. Ph.D. thesis, Institute of Statistics and Decision Sciences, Duke University.
- Lopez, H. F., Salazar, E., & Gamerman, D. (2008). Spatial dynamic factor analysis. *Bayesian Statistics*, 3(4), 759–792.
- Lundeberg, C., Jakobsson, B.-M., & Bonsdorff, E. (2009). The spreading of eutrophication in the eastern coast of the gulf of bothnia northern baltic sea: An analysis in time and space. *Estuarie, Costal and Shelf Science*, 82, 152–160.
- MacKenzie, B. R., Gislason, H., Möllmann, C., & Köster, F. W. (2007). Impact of 21st century climate change on the baltic sea fish community and fisheries. *Global Change Biology*, 13, 1348–1367.
- Mardia, K. V., & Goodall, C. R. (1993). Spatio-temporal analysis of multivariate environmental monitoring data. *Multivariate Environmental Statistics*, (pp. 347–386).
- M.Cingi, S., Keinänen, & Vuorinen, P. J. (2010). Elevated water temperature impairs fertilization and embryonic development of whitefish *Coregonus lavaretus*. *Journal of Fish Biology*, 76, 502–521.
- Meier, H. E. M., Hordoir, R., Andersson, H. C., Dieterich, C., Eilola, K., ..., B. G. G., & Schimanke, S. (2012). Modeling the combined impact of changing climate and changing nutrient loads on the baltic sea environment in an ensemble of transient simulations for 19612099. *Climate Dynamics*, 39, 2421–2441.
- Meriste, M., & Kirsimae, K. (2015). Development of the reed bed in matsalu wetland, estonia: responses to neotectonic land uplift, sea level changes and human influences. *Estonian Journal of Earth Sciences*, 64, 159–172.
- Miller, J. (2010). Species distribution modeling. *Geography Compass*, 4(6), 490–509.
- Müller, R. (1992). Trophic state and its implications for natural reproduction of salmonid fish. In *Dynamics and Use of Lacustrine Ecosystems*. Springer, Dordrecht.
- Nelder, J. A., & Wedderburn, R. W. M. (1972). Generalized linear models. *Journal of the Royal Statistical Association*, 135(3), 370–384.
- Nickisch, H., & Rasmussen, C. E. (2008). Approximations for binary gaussian process classification. *Journal of Machine learning*, 9, 2035–2078.

- Odum, E. P. (1953). *Fundamentals of ecology*. Wiley Subscription Services, Inc., A Wiley Company.
- O'Hagan, A. (1978). Curve fitting and optimal design for prediction. *Journal of Royal Statistical Society B*, 40(1), 1–42.
- Ovaskainen, O., Abrego, N., Halme, P., & Dunson, D. (2016a). Using latent variable models to identify species-to-species associations at different spatial scales. *Methods in Ecology and Evolution*, 7(5), 549–555.
- Ovaskainen, O., Roy, D. B., Fox, R., Fox, R., & Anderson, B. J. (2016b). Uncovering hidden spatial structure in species communities with spatially explicit joint species distribution models. *Methods in Ecology and Evolution*, 7, 428–436.
- Ovaskainen, O., & Soininen, J. (2011). Making more out of sparse data: Hierarchical modelling of species communities. *Ecology*, 92(2), 289–295.
- Ovaskainen, O., Tikhonov, G., Norberg, A., Guillaume Blanchet, F., Duan, L., Dunson, D., Roslin, T., & Abrego, N. (2017). How to make more out of community data? a conceptual framework and its implementation as models and software. *Ecology Letters*, 20(5), 561–576.
- Pauly, D. (1980). On the interrelationships between natural mortality, growth parameters, and mean environmental temperature in 175 fish stocks. *ICES Journal of Marine Science*, 39, 175–192.
- Pearl, J. (2009). Causal inference in statistics: An overview. *Statistics Surveys*, 3, 96–146.
- Peltonen, H., Vinni, M., Lappalainen, A., & Pnni, J. (2004). Spatial feeding patterns of herring (*Clupea harengus* l.), sprat (*Sprattus sprattus* l.), and the three-spined stickleback (emph $Gasterosteus aculeatus$  l.) in the gulf of finland, baltic sea. *ICES Journal of Marine Science*, 61, 966–971.
- Pitkänen, H., Peuraniemi, M., Westerbom, M., Kilpi, M., & von Numers, M. (2013). Longterm changes in distribution and frequency of aquatic vascular plants and charophytes in an estuary in the baltic sea. *Annales Botanica Fennica*, 50, 1e54.
- Pollock, L. J., Tingley, R., Morris, W. K., Golding, N., Hara, R. B. O., Parris, K. M., Vesk, P. A., & McCarthy, M. A. (2014). Understanding co-occurrence by modelling species simultaneously with joint species distribution model (JSDM). *Methods in Ecology and Evolution*, 5, 397–406.
- Rasmussen, C. E., & Williams, C. K. I. (2006). *Gaussian Processes for Machine Learning*. The MIT Press.
- Record, S., Fitzpatrick, M. C., Finley, A. O., Veloz, S., & Ellison, A. M. (2013). Should species distribution models account for spatial autocorrelation? a test of model projections across eight millennia of climate change. *Global Ecology and Biogeography*, 22(6), 760–771.

- Riihimäki, J., & Vehtari, A. (2010). Gaussian processes with monotonicity information. In *AISTATS*, vol. 9, (pp. 645–652).
- Rönnberg, C., & Bonsdorff, E. (2004). Baltic sea eutrophication: area-specific ecological consequences. *Hydrobiologia*, 514, 227–241.
- Rue, H., & Marin, S. (2009). Approximate bayesian inference for latent gaussian models by using integrated laplace approximantions. *Journal of the Royal Statistical Society, Series B*, 71(2), 319–392.
- Shelton, A. O., Thorson, J. T., Ward, E. J., & Feist, B. E. (2014). Spatial semiparametric models improve estimates of species abundance and distribution. *Canadian Journal of Fisheries and Aquatic Sciences*, 71(July), 1655–1666.
- Sieben, K., Ljunggren, L., Bergström, U., & Eriksson, B. K. (2011). A meso-predator release of stickleback promotes recruitment of macroalgae in the baltic sea. *Journal of Experimental Marine Biology and Ecology*, 397, 79e84.
- Snoeijs, P. (1995). Effects of salinity on epiphytic diatom communities on pilayella littoralis (phaeophyceae) in the baltic sea. *Ecoscience*, 2, 382–394.
- Taylor-Rodríguez, D., Kaufeld, K., Schliep, E. M., Clark, J. S., & Gelfand, A. E. (2016). Joint Species Distribution Modeling: Dimension Reduction Using Dirichlet Processes. *Bayesian Analysis*, (pp. 1–29).
- Tokuda, T., Goodrich, B., Mechelen, I. V., & Gelman, A. (2012). Visualizing distributions of covariance matrices.
- Vanhatalo, J., Pietiläinen, V., & Vehtari, A. (2010). Approximate inference for disease mapping with sparse Gaussian processes. *Statistics in Medicine*, 29(15), 1580–1607.
- Vanhatalo, J., Riihimäki, J., Hartikainen, J., Jylänki, P., Tolvanen, V., & Vehtari, A. (2013). GPstuff : Bayesian Modeling with Gaussian Processes. *Journal of Machine Learning Research*, 14, 1175–1179.
- Vanhatalo, J., Veneranta, L., & Hudd, R. (2012). Species distribution modelling with gaussian processes: A case study with youngest stages of sea spawning whitefish (coregonus lavatus l. s.l.) larvae. *Ecological Modelling*, 228, 49–58.
- Vehtari, A., & Ojanen, J. (2012). A survey of bayesian predictive methods for model assessment, selection and comparison. *Statistics Surveys*, 6, 141–228.
- Veneranta, L., Hudd, R., & Vanhatalo, J. (2013). Reproduction areas of sea-spawning coregonids reflect the environment in shallow coastal areas. *Marine Ecology Progress Series*, 477, 231–250.
- Veneranta, L., Urho, L., Lappalainen, A., & Kallasvuo, M. (2011). Turbidity characterizes the reproduction areas of pikeperch (sander lucioperca l.) in the northen baltic sea. *Estuarine, Coastal and Shelf Science*.

- Warton, D. I., Blanchet, F. G., O'Hara, R. B., Ovaskainen, O., Taskinen, S., Walker, S. C., & Hui, F. K. (2015). So Many Variables: Joint Modeling in Community Ecology. *Trends in Ecology and Evolution*, 30(12), 766–779.  
URL <http://dx.doi.org/10.1016/j.tree.2015.09.007>
- Warton, D. I., & Shepherd, L. C. (2010). Poisson point process models solve the "pseudo-absence problem" for presence-only data in ecology. *Annals of Applied Statistics*, 4(3), 1383–1402.
- Wikle, C. K. (2003). Hierarchical models in environmental science. *International Statistical Review*, 71(2), 181–199.
- Yuan, Y., Bachl, F. E., Lindgren, F., Brochers, D. L., Illian, J. B., Buckland, S. T., Rue, H., & Gerrodette, T. (2016). Point process models for spatio-temporal distance sampling data from a large-scale survey of blue whales. 11(4), 2270–2297.  
URL <http://arxiv.org/abs/1604.06013>

## Supplementary material :

### Joint species distribution modeling with additive multi-variate Gaussian process priors and heterogeneous data

Jarno Vanhatalo

*Department of Mathematics and Statistics and Organismal and Evolutionary Biology Research Program, University of Helsinki, Helsinki, Finland*

E-mail: [jarno.vanhatalo@helsinki.fi](mailto:jarno.vanhatalo@helsinki.fi)

Marcelo Hartmann

*Department of Mathematics and Statistics, University of Helsinki, Helsinki, Finland*

E-mail: [marcelo.hartmann@helsinki.fi](mailto:marcelo.hartmann@helsinki.fi)

Lari Veneranta

*Natural Resources Institute Finland, Finland*

E-mail: [lari.veneranta@luke.fi](mailto:lari.veneranta@luke.fi)

#### 1. The posterior expectation and variance for new observations

First we approximate the logistic function with  $p(f) \approx \tilde{p}(f) = a\Phi(f/v_1) + (1-a)\Phi(f/v_2)$  where  $a \in (0, 1)$  and  $v_1, v_2 \in (0, \infty)$  are parameters of the approximation (see Demidenko, 2004). This approximation is used since it has small error bound ( $\leq |10^{-4}|$ , Demidenko (2004)) and can considerably speed-up marginalization over  $f$  for large datasets. Using Lemma 2 in the Section 4, we obtain,

$$\begin{aligned} \mathbb{E}[Y_j(\mathbf{x}_*, \mathbf{s}_*) | \mathbf{y}, \boldsymbol{\eta}, \Lambda] &= z_{j,*} a\Phi\left(\frac{\mu_{j,*}}{\sqrt{\Sigma_{j,*} + v_1^2}}\right) + z_{j,*} (1-a)\Phi\left(\frac{\mu_{j,*}}{\sqrt{\Sigma_{j,*} + v_2^2}}\right) \quad (1) \\ \mathbb{V}[Y_j(\mathbf{x}_*, \mathbf{s}_*) | \mathbf{y}, \boldsymbol{\eta}, \Lambda] &= \mathbb{E}[Y_j(\mathbf{x}_*, \mathbf{s}_*) | \mathbf{y}, \boldsymbol{\eta}, \Lambda] - \mathbb{E}[Y_j(\mathbf{x}_*, \mathbf{s}_*) | \mathbf{y}, \boldsymbol{\eta}, \Lambda]^2 \\ &\quad + (z_{j,*}^2 - z_{j,*})\mathbb{E}[\tilde{p}^2(f_*)] \end{aligned}$$

where,  $\Phi(\cdot)$  is the cumulative distribution of the standard Gaussian random variable and

$$\mathbb{E}[\tilde{p}^2(f_*)] = a^2 F_2(\boldsymbol{\mu}_{j,*} | V_{1,1}) + (1-a)^2 F_2(\boldsymbol{\mu}_{j,*} | V_{2,2}) + 2a(1-a)F_2(\boldsymbol{\mu}_{j,*} | V_{1,2}) \quad (2)$$

$F_2(\boldsymbol{\mu}_{j,*} | V_{m,n})$  is the zero-mean 2-dimensional Gaussian cumulative distribution function evaluated at  $\boldsymbol{\mu}_{j,*} = [\mu_{j,*} \ \mu_{j,*}]^T$  with covariance matrix given by

$$V_{m,n} = \begin{bmatrix} \Sigma_{j,*} + v_m^2 & \Sigma_{j,*} \\ \Sigma_{j,*} & \Sigma_{j,*} + v_n^2 \end{bmatrix}. \quad (3)$$

In the case of Negative-Binomial model, we use the moment generating function of a Gaussian random variable to obtain the unconditional expectation of a future outcome

w.r.t to latent variable, i.e.

$$\begin{aligned}\mathbb{E}[Y_j(\mathbf{x}_*, \mathbf{s}_*) | \mathbf{y}, \boldsymbol{\eta}, \Lambda] &= z_{j,*} e^{\mu_{j,*} + \Sigma_{j,*}/2} \\ \mathbb{V}[Y_j(\mathbf{x}_*, \mathbf{s}_*) | \mathbf{y}, \boldsymbol{\eta}, \Lambda] &= z_{j,*}^2 e^{\mu_{j,*} + \Sigma_{j,*}/2} + z_{j,*}^2 e^{2\mu_{j,*} + \Sigma_{j,*}} \left[ e^{\Sigma_{j,*}/2} (\hat{r}_j + 1)/\hat{r}_j - 1 \right].\end{aligned}\quad (4)$$

## 2. Conditional predictions

Recall that, in the main paper, the distribution of  $\mathbf{Y}_{\mathcal{J}_1}(\mathbf{x}_*, \mathbf{s}_*) | \mathbf{y}_{\mathcal{J}_2}$  conditioned on hyperparameters (they were omitted from the notation for simplicity) is given by

$$\pi(\mathbf{y}_{\mathcal{J}_1,*} | \mathbf{y}_{\mathcal{J}_2}) = \int \pi(\mathbf{y}_{\mathcal{J}_1,*} | \mathbf{y}_{\mathcal{J}_2}, \mathbf{f}_{\mathcal{J}_1,*}) \pi(\mathbf{y}_{\mathcal{J}_2}, \mathbf{f}_{\mathcal{J}_1,*}) d\mathbf{f}_{\mathcal{J}_1,*} / \pi(\mathbf{y}_{\mathcal{J}_2}) \quad (5)$$

The second term in the numerator of the integrand of (5) is the same as,

$$\pi(\mathbf{y}_{\mathcal{J}_2}, \mathbf{f}_{\mathcal{J}_1,*}) = \int \pi(\mathbf{f}_{\mathcal{J}_1,*} | \mathbf{f}_{\mathcal{J}_2}, \mathbf{y}_{\mathcal{J}_2}) \pi(\mathbf{f}_{\mathcal{J}_2} | \mathbf{y}_{\mathcal{J}_2}) \pi(\mathbf{y}_{\mathcal{J}_2}) d\mathbf{f}_{\mathcal{J}_2}. \quad (6)$$

Now,  $\mathbf{f}_{\mathcal{J}_1,*} | \mathbf{f}_{\mathcal{J}_2}, \mathbf{y}_{\mathcal{J}_2}$  also only depends on  $\mathbf{f}_{\mathcal{J}_2}$ . Plugging (6) into (5) we get

$$\pi(\mathbf{y}_{\mathcal{J}_1,*} | \mathbf{y}_{\mathcal{J}_2}) = \int \pi(\mathbf{y}_{\mathcal{J}_1,*} | \mathbf{f}_{\mathcal{J}_1,*}) \pi(\mathbf{f}_{\mathcal{J}_1,*} | \mathbf{f}_{\mathcal{J}_2}) \pi(\mathbf{f}_{\mathcal{J}_2} | \mathbf{y}_{\mathcal{J}_2}) d\mathbf{f}_{\mathcal{J}_2} d\mathbf{f}_{\mathcal{J}_1,*} \quad (7)$$

where last two terms in (7) are Gaussians. The first one is the conditional Gaussian density function w.r.t. the predictor function values  $\mathbf{f}_{\mathcal{J}_2}$ , that is,  $\pi(\mathbf{f}_{\mathcal{J}_1,*} | \mathbf{f}_{\mathcal{J}_2}) = \mathcal{N}(\mathbf{f}_{\mathcal{J}_1,*} | C_{\mathcal{J}_1, \mathcal{J}_2*} C_{\mathcal{J}_2, \mathcal{J}_2}^{-1} \mathbf{f}_{\mathcal{J}_2}, C_{\mathcal{J}_1, \mathcal{J}_2*} - C_{\mathcal{J}_1, \mathcal{J}_2*} C_{\mathcal{J}_2, \mathcal{J}_2}^{-1} C_{\mathcal{J}_1, \mathcal{J}_2*}^T)$  and the second one is the Laplace approximation using the *scenario species data* related to the set  $\mathcal{J}_2$ , that is,  $\pi(\mathbf{f}_{\mathcal{J}_2} | \mathbf{y}_{\mathcal{J}_2}) \approx \mathcal{N}(\mathbf{f}_{\mathcal{J}_2} | C_{\mathcal{J}_2, \mathcal{J}_2} \nabla \log \pi(\mathbf{y}_{\mathcal{J}_2} | \hat{\mathbf{f}}_{\mathcal{J}_2}), (C_{\mathcal{J}_2, \mathcal{J}_2}^{-1} + W_{\mathcal{J}_2})^{-1})$ . Plugging this approximate density function in the equation (7) gives

$$\pi(\mathbf{y}_{\mathcal{J}_1,*} | \mathbf{y}_{\mathcal{J}_2}) = \int \pi(\mathbf{y}_{\mathcal{J}_1,*} | \mathbf{f}_{\mathcal{J}_1,*}) \mathcal{N}(\mathbf{f}_{\mathcal{J}_1,*} | \mu_{|\mathcal{J}_2}, \Sigma_{|\mathcal{J}_2}) d\mathbf{f}_{\mathcal{J}_1,*} \quad (8)$$

with

$$\begin{aligned}\mu_{|\mathcal{J}_2} &= C_{\mathcal{J}_1, \mathcal{J}_2*} \nabla \log \pi(\mathbf{y}_{\mathcal{J}_2} | \hat{\mathbf{f}}_{\mathcal{J}_2}) \\ \Sigma_{|\mathcal{J}_2} &= C_{\mathcal{J}_1, \mathcal{J}_2*} - C_{\mathcal{J}_1, \mathcal{J}_2*} (C_{\mathcal{J}_2, \mathcal{J}_2} + W_{\mathcal{J}_2}^{-1})^{-1} C_{\mathcal{J}_1, \mathcal{J}_2*}^T\end{aligned}\quad (9)$$

where  $C_{\mathcal{J}_1, \mathcal{J}_2*}$  is the covariance between species in the set  $\mathcal{J}_1$  at the point  $(\mathbf{x}_*, \mathbf{s}_*)$  and the species in the set  $\mathcal{J}_2$  in their respective covariates and spatial locations.  $\nabla \log \pi(\mathbf{y}_{\mathcal{J}_2} | \hat{\mathbf{f}}_{\mathcal{J}_2})$  correspond to the gradient of the log-likelihood function for species related to the set  $\mathcal{J}_2$ .  $C_{\mathcal{J}_1, \mathcal{J}_2*}$  is the covariance matrix of  $\mathbf{f}_{\mathcal{J}_1,*}$  at  $(\mathbf{x}_*, \mathbf{s}_*)$ .  $C_{\mathcal{J}_2, \mathcal{J}_2}$  is the covariance matrix of  $\mathbf{f}_{\mathcal{J}_2}$  and  $W_{\mathcal{J}_2}$  is the negative Hessian matrix of the negative logarithm of the likelihood functions related to species in the set  $\mathcal{J}_2$ . Now, to calculate the predictive mean vector and predictive covariance matrix we follow the steps used in deriving unconditional expectation and unconditional variances as in the main paper. However we exclude them for brevity.

### 3. Unconstrained parametrization of covariance matrices

Let the matrix  $\Sigma$  be a covariance matrix of dimension  $J$ . In terms of variances and correlations, we rewrite  $\Sigma = \text{diag}(\sigma_1^2, \dots, \sigma_J^2)^{\frac{1}{2}} \mathcal{P} \text{diag}(\sigma_1^2, \dots, \sigma_J^2)^{\frac{1}{2}}$ , where  $\sigma_j^2, j = 1, \dots, J$  are variances and these are transformed as  $\sigma_j^2 = \exp(\delta_j)$ . The correlation matrix  $\mathcal{P}$  is written in terms of its Cholesky decomposition, that is  $\mathcal{P} = LL^T$ , where  $L$  is the lower triangular Cholesky decomposition. In our case, the upper triangular Cholesky decomposition is given by

$$L^T = \begin{bmatrix} 1 & z_{1,2} & z_{1,3} & \cdots & z_{1,J} \\ 0 & \prod_{i=1}^1 (1 - z_{i,2}^2)^{\frac{1}{2}} & z_{2,3} \prod_{i=1}^1 (1 - z_{i,3}^2)^{\frac{1}{2}} & \cdots & z_{2,J} \prod_{i=1}^1 (1 - z_{i,J}^2)^{\frac{1}{2}} \\ \vdots & \vdots & \vdots & \ddots & \vdots \\ 0 & 0 & 0 & \cdots & \prod_{i=1}^{J-1} (1 - z_{i,J}^2)^{\frac{1}{2}} \end{bmatrix} \quad (10)$$

where each  $z_{i,i'} \in (-1, 1)$ . Now, since each  $z_{i,i'}$  can freely vary in the interval  $(-1, 1)$  without violate the positive definiteness property of  $\mathcal{P}$  (see Kurowicka and Cooke, 2003; Lewandowski et al., 2009), we map each  $z_{i,i'}$  to the real line as  $z_{i,i'} = 2/[1 + \exp(-a\delta_{i,i'})] - 1$ , where  $\delta_{i,i'} \in \mathbb{R}$ .

The derivative of the  $\log \pi(\mathcal{P})$  (recall the prior for the correlation matrix in the main paper) w.r.t. each  $\delta_{i,i'}$  is given by

$$\frac{\partial}{\partial \delta_{i,i'}} \log \pi(\mathcal{P} | v) = \sum_{j=1}^{J-1} \sum_{j'=j+1}^J \frac{\partial}{\partial \rho_{j,j'}} \log \pi(\mathcal{P} | v) \frac{\partial}{\partial \delta_{i,i'}} \rho_{j,j'} \quad (11)$$

and the partial derivatives of  $\log \pi(\mathcal{P} | v)$  w.r.t to  $\rho_{j,j'}$  are obtained as,

$$\frac{\partial}{\partial \rho_{j,j'}} \log \pi(\mathcal{P} | v) = ((v-1)(J-1) - 1) \{\mathcal{P}^{-1}\}_{j,j'} - v \sum_{\substack{r=1 \\ r \notin \{j,j'\}}}^J \{\mathcal{P}_{rr}^{-1}\}_{c,c'} \quad (12)$$

where  $c = j-1$  and  $c' = j'$  if  $r < j$  and,  $j' = 1$  or  $r > j'$ . If  $r < j$  and  $r < j'$  then  $c = j-1$  and  $c' = j'-1$ .  $\{\mathcal{P}^{-1}\}_{j,j'}$  is the entry  $(j, j')$  of the matrix  $\mathcal{P}^{-1}$  and  $\{\mathcal{P}_{rr}^{-1}\}_{c,c'}$  is the entry  $(c, c')$  of the inverse matrix  $\mathcal{P}_{rr}^{-1}$ , where  $\mathcal{P}_{rr}$  is a matrix obtained by removing the  $r$ 'th row and column of  $\mathcal{P}$ . The partial derivatives of each  $\rho_{j,j'}$  w.r.t to  $\delta_{i,i'}$  are obtained from  $\partial \mathcal{P} / \partial \delta_{i,i'} = (\partial L / \partial \delta_{i,i'}) L^T + L (\partial L / \partial \delta_{i,i'})^T$ .

Lastly, we find the derivatives of the logarithm of the absolute value of the Jacobian determinant w.r.t each  $\delta_{i,i'}$  (see equation (11) in Lewandowski et al. 2009).

$$\begin{aligned} \frac{\partial}{\partial \delta_{i,i'}} \log \left| \frac{\partial(\rho_{1,2}, \dots, \rho_{J-1,J})}{\partial(\delta_{1,2}, \dots, \delta_{J-1,J})} \right| &= \frac{\partial}{\partial \delta_{i,i'}} \log \prod_{j=1}^{J-1} \prod_{j'=j+1}^J (1 - z_{j,j'}^2)^{(J-j-1)/2} \frac{dz_{j,j'}}{d\delta_{j,j'}} \\ &= -(J-i-1) \frac{z_{i,i'}}{1 - z_{i,i'}^2} \frac{dz_{i,i'}}{d\delta_{i,i'}} + \frac{d^2 z_{i,i'}/d\delta_{i,i'}^2}{dz_{i,i'}/d\delta_{i,i'}} \end{aligned} \quad (13)$$

#### 4. Gaussian integrals

LEMMA 1. Let's denote by  $\Phi(\cdot)$  the standard-Gaussian cumulative distribution function and  $\mathcal{N}(\cdot|\mu, \sigma^2)$  the Gaussian density function with parameters  $(\mu, \sigma^2) \in \mathbb{R} \times \mathbb{R}_+$ . Then the following holds

$$\int_{-\infty}^{\infty} \mathcal{N}(x|\mu, \sigma^2) \prod_{r=1}^N \Phi\left(\frac{x - m_r}{v_r}\right) dx = F_N(\boldsymbol{\mu}_N | \mathbf{m}_N, V_N) \quad (14)$$

where  $F_N(\cdot|\mathbf{c}, \mathcal{C})$  is the  $N$ -dimensional Gaussian cumulative distribution function with parameters  $(\mathbf{c}, \mathcal{C}) \in \mathbb{R}^N \times \mathcal{R}$ , with  $\mathcal{R}$  the space of positive-definite matrices (covariance matrices). Furthermore,  $\mathbf{m}_N = [m_1 \dots m_N]^T \in \mathbb{R}^N$ ,  $\boldsymbol{\mu}_N = \mu \mathbf{1}_N \in \mathbb{R}^N$ ,  $v_r > 0 \ \forall r$  and  $V_N$  is a covariance matrix given by,

$$V_N = \begin{bmatrix} v_1^2 + \sigma^2 & \dots & \sigma^2 \\ \vdots & \ddots & \vdots \\ \sigma^2 & \dots & v_N^2 + \sigma^2 \end{bmatrix} \quad (15)$$

PROOF. To show (14), start writing the left-hand side of the equation in full. Rewrite the integrand as the product of non-standard Gaussian density functions as well as the regions of integration, i.e.,

$$\int_{-\infty}^{\infty} \int_{-\infty}^x \dots \int_{-\infty}^x \mathcal{N}(y_1|m_1, v_1^2) \dots \mathcal{N}(y_N|m_N, v_N^2) \mathcal{N}(x|\mu, \sigma^2) dy_1 \dots dy_N dx. \quad (16)$$

Rewrite again using the following transformation  $[x, y_1, \dots, y_N]^T = [w + \mu, z_1 + w + m_1, \dots, z_N + w + m_N]^T$  and note that  $|\partial(x, y_1, \dots, y_N)/\partial(w, z_1, \dots, z_N)| = 1$ . After changing variables, group the different terms in the exponentials together to have

$$\int_{-\infty}^{\infty} \int_{-\infty}^{\mu-m_N} \dots \int_{-\infty}^{\mu-m_1} \frac{1}{c} \exp \left\{ -\frac{1}{2} \left[ \sum_{r=1}^N \frac{(z_r+w)^2}{v_r^2} + \frac{w^2}{\sigma^2} \right] \right\} dz_1 \dots dz_N dw \quad (17)$$

where  $c = \sigma(2\pi)^{(N+1)/2} \prod_{r=1}^N v_r$ . Now, the expression inside the squared bracket is a

quadratic form which is written with the following matrix form,

$$\begin{aligned}
\sum_{r=1}^N \frac{(z_r+w)^2}{v_r^2} + \frac{w^2}{\sigma^2} &= w^2 \left( \sum_{r=1}^N \frac{1}{v_r^2} + \frac{1}{\sigma^2} \right) + w \sum_{r=1}^N \frac{z_r}{v_r^2} + \sum_{r=1}^N z_r \left( \frac{w}{v_r^2} + \frac{z_r}{v_r^2} \right) \\
&= \begin{bmatrix} w \left( \sum_{r=1}^N \frac{1}{v_r^2} + \frac{1}{\sigma^2} \right) + \sum_{r=1}^N \frac{z_r}{v_r^2} \\ \frac{w}{v_1^2} + \frac{z_1}{v_1^2} \\ \vdots \\ \frac{w}{v_N^2} + \frac{z_N}{v_N^2} \end{bmatrix}^T \begin{bmatrix} w \\ z_1 \\ \vdots \\ z_N \end{bmatrix} \\
&= \begin{bmatrix} w \\ z_1 \\ \vdots \\ z_N \end{bmatrix}^T \begin{bmatrix} \sum_{r=1}^N \frac{1}{v_r^2} + \frac{1}{\sigma^2} & \frac{1}{v_1^2} & \cdots & \frac{1}{v_N^2} \\ \frac{1}{v_1^2} & \frac{1}{v_1^2} & \cdots & 0 \\ \vdots & \vdots & \ddots & \vdots \\ \frac{1}{v_N^2} & 0 & \cdots & \frac{1}{v_N^2} \end{bmatrix} \begin{bmatrix} w \\ z_1 \\ \vdots \\ z_N \end{bmatrix} \tag{18}
\end{aligned}$$

therefore (17) is the same as

$$\int_{-\infty}^{\infty} \int_{-\infty}^{\mu-m_N} \cdots \int_{-\infty}^{\mu-m_1} \frac{1}{c} \exp \left\{ -\frac{1}{2} \begin{bmatrix} w \\ z_1 \\ \vdots \\ z_N \end{bmatrix}^T \begin{bmatrix} \sum_{r=1}^N \frac{1}{v_r^2} + \frac{1}{\sigma^2} & \frac{1}{v_1^2} & \cdots & \frac{1}{v_N^2} \\ \frac{1}{v_1^2} & \frac{1}{v_1^2} & \cdots & 0 \\ \vdots & \vdots & \ddots & \vdots \\ \frac{1}{v_N^2} & 0 & \cdots & \frac{1}{v_N^2} \end{bmatrix} \begin{bmatrix} w \\ z_1 \\ \vdots \\ z_N \end{bmatrix} \right\} d\mathbf{z} dw \tag{19}$$

The integrand in (19) has the full form of the multivariate Gaussian density. To identify this we need to find the closed-form covariance matrix from the precision matrix in (19) and show that the determinant of the covariance matrix is given by  $c^2/(2\pi)^{N+1}$ . Write the precision matrix as block matrix such that  $A = \sum_{r=1}^N \frac{1}{v_r^2} + \frac{1}{\sigma^2}$ ,  $B = \begin{bmatrix} \frac{1}{v_1^2} & \cdots & \frac{1}{v_N^2} \end{bmatrix}$ ,  $C = B^T$  and  $D = \text{diag} \left( \frac{1}{v_1^2}, \dots, \frac{1}{v_N^2} \right)$ . Use the partitioned matrix inversion lemma (Strang and Borre, 1997, equation 17.44) to get the blocks,  $(A - BD^{-1}C)^{-1} = \sigma^2$ ,  $(BD^{-1}C - A)^{-1}BD^{-1} = -\sigma^2[1 \cdots 1]$ ,  $D^{-1}C(BD^{-1}C - A)^{-1} = -\sigma^2[1 \cdots 1]^T$  and  $D^{-1} + D^{-1}C(A - BD^{-1}C)^{-1}BD^{-1}$  where its main diagonal equals to  $[v_1^2 + \sigma^2, \dots, v_N^2 + \sigma^2]$  and all off-diagonal elements are given by  $\sigma^2$ . Put everything together to have the covariance matrix

$$\begin{bmatrix} \sigma^2 & -\sigma^2 & \cdots & -\sigma^2 \\ -\sigma^2 & v_1^2 + \sigma^2 & \cdots & \sigma^2 \\ -\sigma^2 & \vdots & \ddots & \vdots \\ -\sigma^2 & \sigma^2 & \cdots & v_N^2 + \sigma^2 \end{bmatrix} \tag{20}$$

whose determinant equals to  $1/[\det(D) \det(A - BD^{-1}C)] = \sigma^2 \prod_{r=1}^N v_r^2 = c^2/(2\pi)^{N+1}$  by the partitioned matrix determinant lemma (e.g., Rasmussen and Williams, 2006). Finally, in (19), interchange the order of integration with Fubini-Tonelli theorem (Folland,

2013) and integrate w.r.t.  $w$  to get

$$\int_{-\infty}^{\mu-m_N} \cdots \int_{-\infty}^{\mu-m_1} \mathcal{N} \left( \begin{bmatrix} z_1 \\ \vdots \\ z_N \end{bmatrix} \middle| \begin{bmatrix} 0 \\ \vdots \\ 0 \end{bmatrix}, \begin{bmatrix} v_1^2 + \sigma^2 & \cdots & \sigma^2 \\ \vdots & \ddots & \vdots \\ \sigma^2 & \cdots & v_N^2 + \sigma^2 \end{bmatrix} \right) dz_1 \cdots dz_N \quad (21)$$

that equals to

$$F_N \left( \begin{bmatrix} \mu \\ \vdots \\ \mu \end{bmatrix} \middle| \begin{bmatrix} m_1 \\ \vdots \\ m_N \end{bmatrix}, \begin{bmatrix} v_1^2 + \sigma^2 & \cdots & \sigma^2 \\ \vdots & \ddots & \vdots \\ \sigma^2 & \cdots & v_N^2 + \sigma^2 \end{bmatrix} \right) \quad (22)$$

and therefore the equality (14) holds.

LEMMA 2. *Let  $\mathcal{N}(\cdot | \boldsymbol{\mu}_N, \Sigma)$  be the  $N$ -dimensional Gaussian density function with mean parameter  $\boldsymbol{\mu}_N$  and covariance matrix  $\Sigma$ . Then the following holds true,*

$$\int_{\mathbb{R}^N} F_N(\mathbf{x} | \mathbf{m}_N, \mathbf{V}) \mathcal{N}(\mathbf{x} | \boldsymbol{\mu}_N, \Sigma) d\mathbf{x} = F_N(\boldsymbol{\mu}_N | \mathbf{m}_N, \mathbf{V} + \Sigma) \quad (23)$$

where  $F_N(\cdot | \mathbf{c}, \mathcal{C})$  is the  $N$ -dimensional Gaussian cumulative distribution function with parameters  $(\mathbf{c}, \mathcal{C})$ . Furthermore,  $\mathbf{m}_N = [m_1 \cdots m_N]^T \in \mathbb{R}^N$ ,  $\boldsymbol{\mu}_N = [\mu_1 \cdots \mu_N]^T \in \mathbb{R}^N$ ,  $\mathbf{V}$  and  $\Sigma$  are covariance matrices.

PROOF. Let's rewrite the left-hand side of (23) in full,

$$\int_{\mathbb{R}^N} \int_{-\infty}^{x_n} \cdots \int_{-\infty}^{x_1} \mathcal{N}(\mathbf{y} | \mathbf{m}, \mathbf{V}) \mathcal{N}(\mathbf{x} | \boldsymbol{\mu}_N, \Sigma) d\mathbf{y} d\mathbf{x} \quad (24)$$

where  $\mathbf{y} = [y_1, \cdots, y_N]^T$ . Let's use the following transformation  $[x_1, \cdots, x_N, y_1, \cdots, y_N]^T = [w_1 + \mu_1, \cdots, w_N + \mu_N, z_1 + w_1 + m_1, \cdots, z_N + w_N + m_N]^T$ . The Jacobian of this transformation simplifies to  $|\partial(x_1, \cdots, x_N, y_1, \cdots, y_N) / \partial(w_1, \cdots, w_N, z_1, \cdots, z_N)| = 1$ . Rewrite the above equation to get,

$$\int_{\mathbb{R}^N} \int_{-\infty}^{\mu_N-m_N} \cdots \int_{-\infty}^{\mu_1-m_1} \mathcal{N}(\mathbf{w} | \mathbf{z}, \mathbf{V}) \mathcal{N}(\mathbf{w} | \mathbf{0}, \Sigma) d\mathbf{z} d\mathbf{w} \quad (25)$$

where  $\mathbf{z} = [z_1 \cdots z_N]^T$  and  $\mathbf{w} = [w_1 \cdots w_N]^T$ . Note that the product of two multivariate Gaussian density functions is another unnormalized multivariate Gaussian (see, e.g., Rasmussen and Williams, 2006, Appendix A). Therefore we write

$$\int_{\mathbb{R}^N} \int_{-\infty}^{\mu_N-m_N} \cdots \int_{-\infty}^{\mu_1-m_1} \mathcal{N}(\mathbf{z} | \mathbf{0}, \mathbf{V} + \Sigma) \mathcal{N}(\mathbf{w} | \mathbf{c}, \mathcal{C}) d\mathbf{z} d\mathbf{w} \quad (26)$$

where  $c = -CV^{-1}\mathbf{z}$  and  $C = (V^{-1} + \Sigma^{-1})^{-1}$ . Interchange the order of integration with Fubini-Tonelli theorem (Folland, 2013) and integrate w.r.t  $\mathbf{w}$  to get that,

$$\int_{-\infty}^{\mu_N - m_N} \cdots \int_{-\infty}^{\mu_1 - m_1} \mathcal{N}(\mathbf{z} | \mathbf{0}, V + \Sigma) d\mathbf{z} = F_N(\boldsymbol{\mu}_N | \mathbf{m}_N, V + \Sigma) \quad (27)$$

which completes the proof.

The above closed-form integrals extend many equalities in the table of Owen (1980).

## References

- Demidenko, E. (2004) *Mixed Models: Theory and Application*. John Wiley & Sons.
- Folland, G. (2013) *Real Analysis: Modern Techniques and Their Applications*. Pure and Applied Mathematics: A Wiley Series of Texts, Monographs and Tracts. Wiley.
- Kurowicka, D. and Cooke, R. (2003) A parameterization of positive definite matrices in terms of partial correlation vines. *Linear Algebra and its Applications*, **372**, 225–251.
- Lewandowski, D., Kurowicka, D. and Joe, H. (2009) Generating random correlation matrices based on vines and extended onion method. *Journal of Multivariate Analysis*, **100**, 1989–2001.
- Owen, D. B. (1980) A table of normal integrals. *Communications in Statistics - Simulation and Computation*, **9**, 389–419. URL: <http://dx.doi.org/10.1080/03610918008812164>.
- Rasmussen, C. E. and Williams, C. K. I. (2006) *Gaussian Processes for Machine Learning*. The MIT Press.
- Strang, G. and Borre, K. (1997) *Linear Algebra, Geodesy and GPS*. Wellesley-Cambridge Press.

**Table 1.** Hyperparameters estimate from covariates covariance functions

	Diatom-algae		Filam-algae		Macro-veg		Threespine-sb		Ninespine-sb		White-fish		Vendance		
	SDM   JSDM														
Variances															
Length-scales	$\hat{\sigma}_S^2$	$\hat{\sigma}_J^2$													
	$\hat{\ell}_S^2$	$\hat{\ell}_J^2$													
Openness	$\sigma^2$	1.92	2.19	1.96	1.87	1.63	1.62	1.70	1.64	2.18	1.78	1.57	1.30	2.61	2.47
	$\ell$	1.56	1.59	1.29	1.31	1.51	1.26	1.90	2.23	2.12	1.86	1.98	1.61	0.64	0.92
Distance to deep	$\sigma^2$	2.24	1.84	1.55	1.48	2.87	2.64	2.54	2.23	1.98	1.43	1.66	1.32	1.79	1.37
	$\ell$	1.09	1.18	1.16	1.06	1.39	1.87	1.04	1.39	1.48	1.80	2.02	1.33	1.32	1.09
Sandy bottom index	$\sigma^2$	1.89	1.72	1.51	1.63	2.14	1.85	2.11	1.49	1.89	1.79	3.37	2.26	2.59	2.37
	$\ell$	1.49	1.43	1.48	1.24	1.30	0.84	0.71	0.46	1.93	1.60	1.15	0.95	0.91	1.06
Ice breakup week	$\sigma^2$	2.36	2.37	2.16	1.74	3.26	2.54	1.70	1.63	1.99	1.86	1.64	1.09	6.69	7.52
	$\ell$	1.11	1.18	0.75	1.06	0.62	1.87	1.32	1.39	2.22	1.80	1.87	1.33	0.70	1.09
Chlorophyl-a	$\sigma^2$	1.62	1.53	1.55	1.64	2.93	2.68	1.91	1.46	1.72	1.42	1.95	1.75	2.53	2.48
	$\ell$	1.11	1.46	0.75	0.78	0.62	0.49	1.32	1.76	2.22	1.71	1.87	1.30	0.70	0.66
Distance to nearest river	$\sigma^2$	1.68	1.42	1.56	1.30	1.69	2.26	1.96	1.71	1.90	2.34	1.67	2.67	1.65	1.55
	$\ell$	1.59	1.76	1.63	1.42	1.10	0.80	0.76	0.65	1.23	0.73	0.36	0.41	1.45	1.63
Bottom type	$\sigma^2$	0.81	1.01	0.69	1.07	0.69	0.81	1.77	0.87	1.08	1.00	2.01	1.00	0.75	1.00
Salinity	$\sigma^2$													2.87	2.17
	$\ell$													1.24	1.37
Spatial	$\sigma^2$	10.9	9.35	7.31	6.00	4.62	4.67	6.87	6.42	5.66	5.74	8.11	7.39	9.32	6.85
	$\ell$	0.47	0.45	0.74	1.06	0.61	0.44	0.44	0.43	0.78	0.95	0.15	0.22	2.14	2.45

### A. Figures

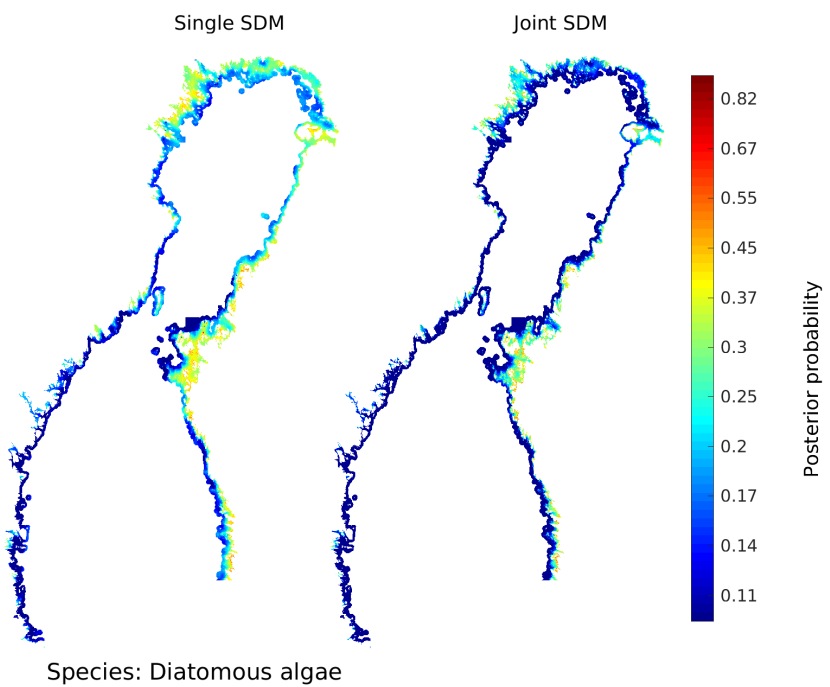


**Fig. 1.** Posterior predictive median of intensity and the expected count of individuals in replicate sampling for diatomo algae.

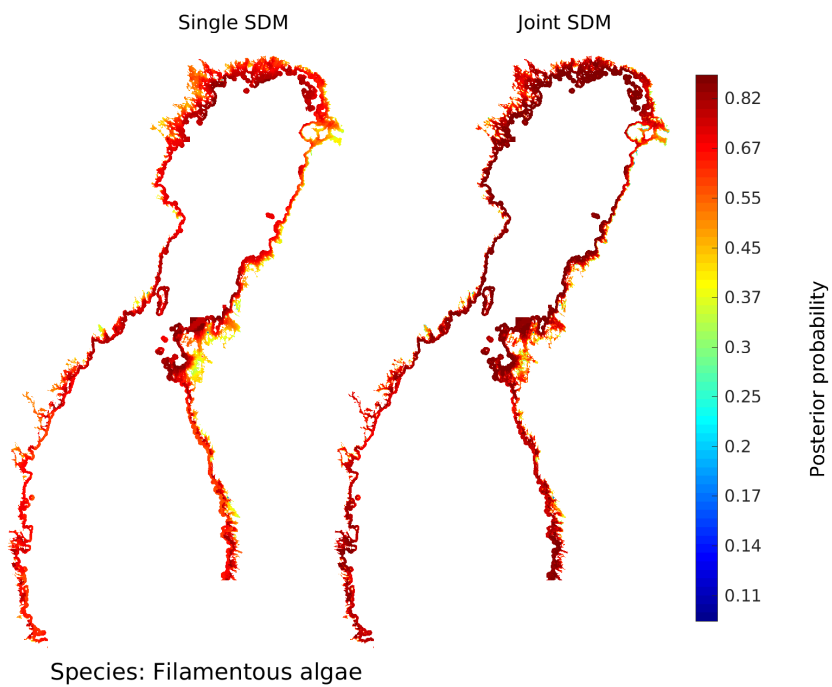


**Fig. 2.** Posterior predictive median of intensity and the expected count of individuals in replicate sampling for filamentous algae.

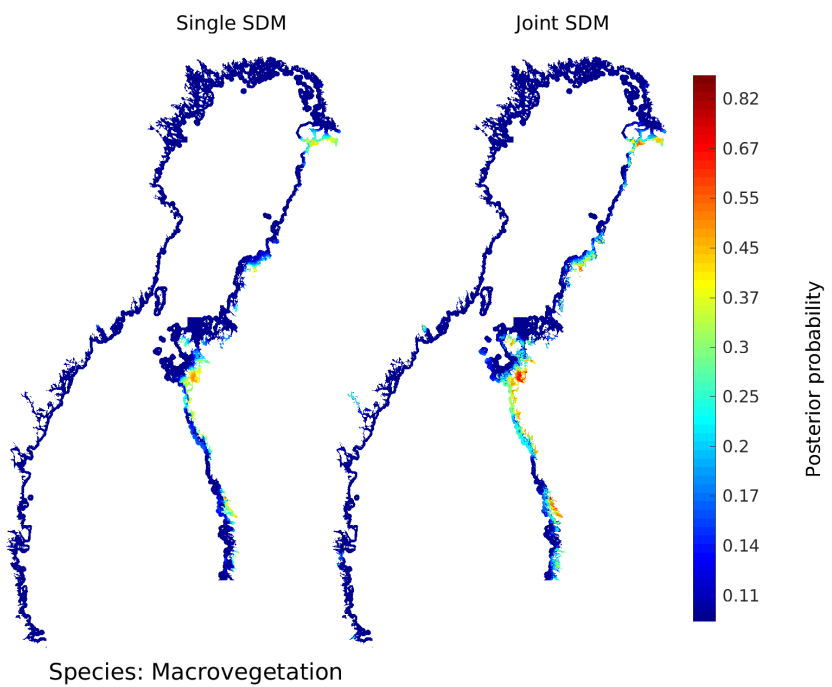


**Fig. 3.** Posterior predictive median of intensity and the expected count of individuals in replicate sampling for macrovegetation.

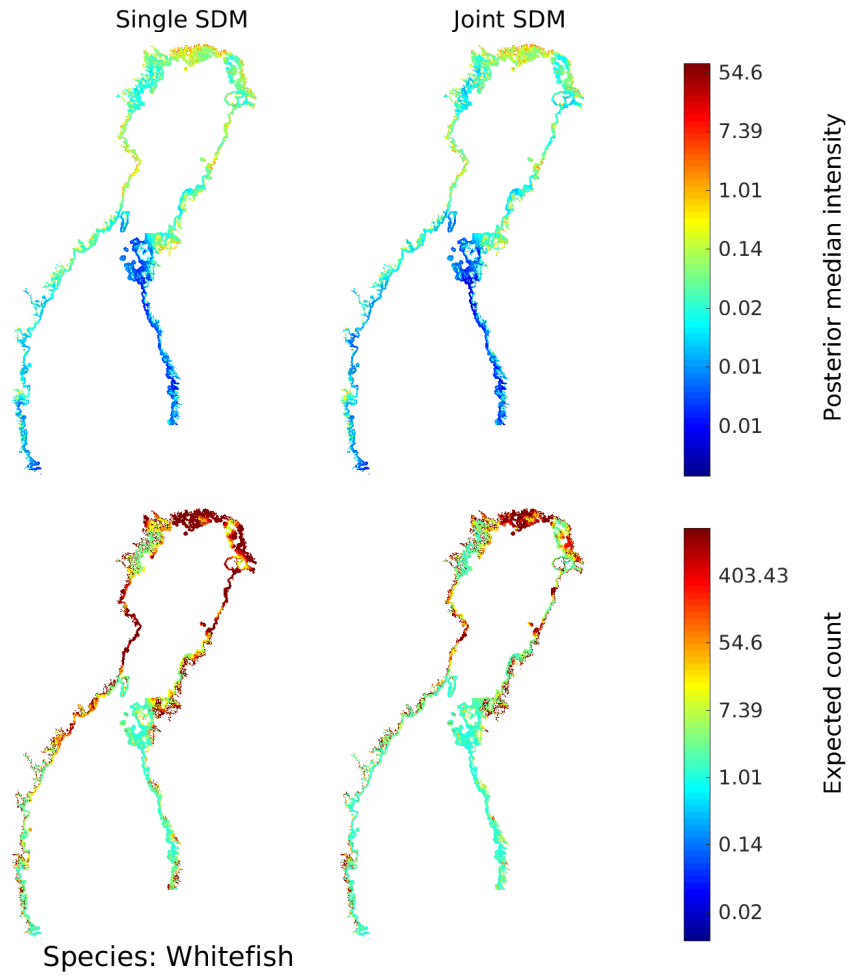


**Fig. 4.** Posterior predictive median of intensity and the expected count of individuals in replicate sampling for whitefish.

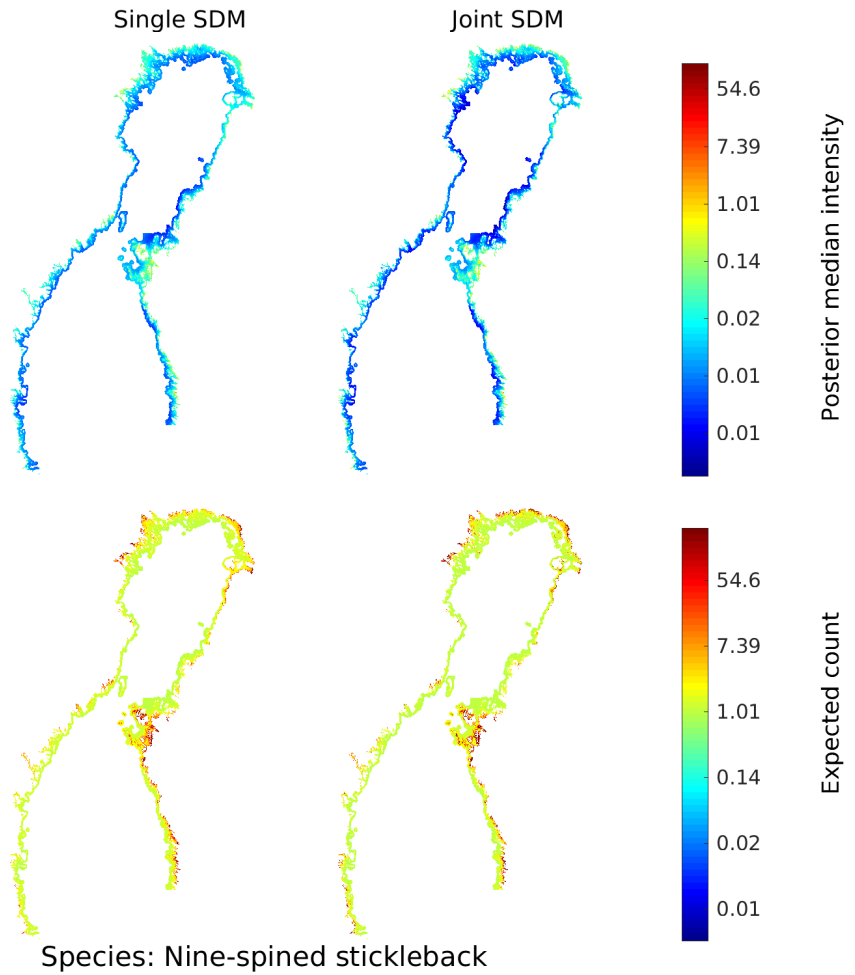


**Fig. 5.** Posterior predictive median of intensity and the expected count of individuals in replicate sampling for ninespine-stickleback.

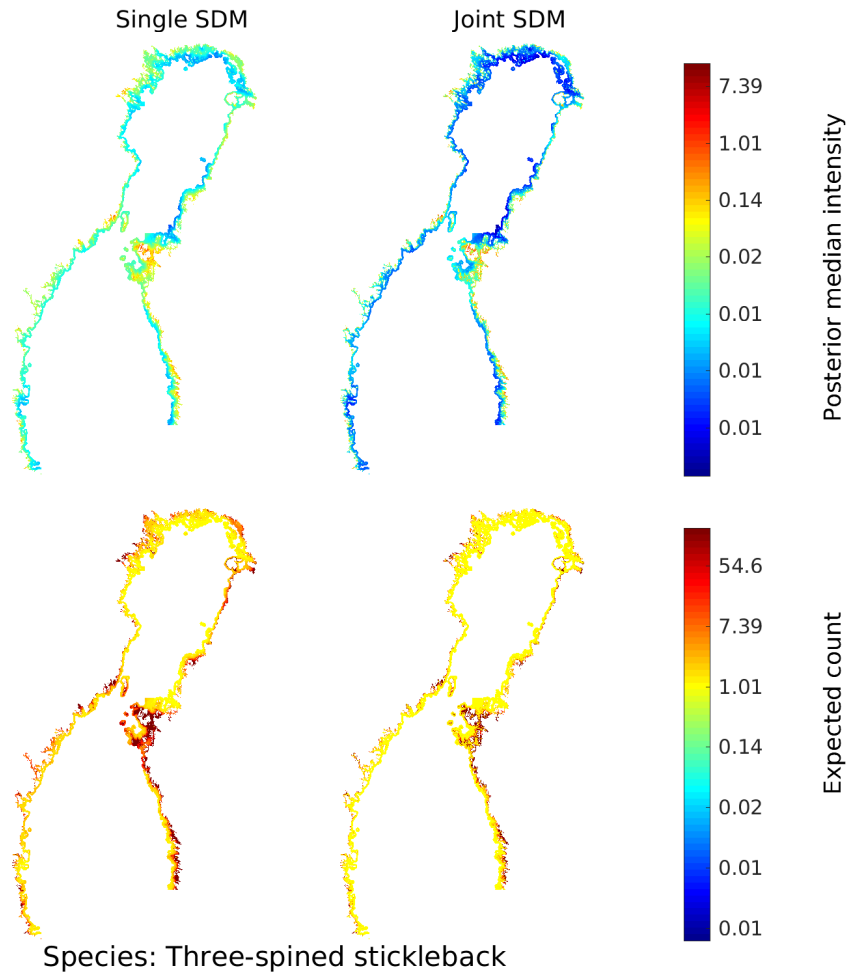


**Fig. 6.** Posterior predictive median of intensity and the expected count of individuals in replicate sampling for threespine-stickleback.

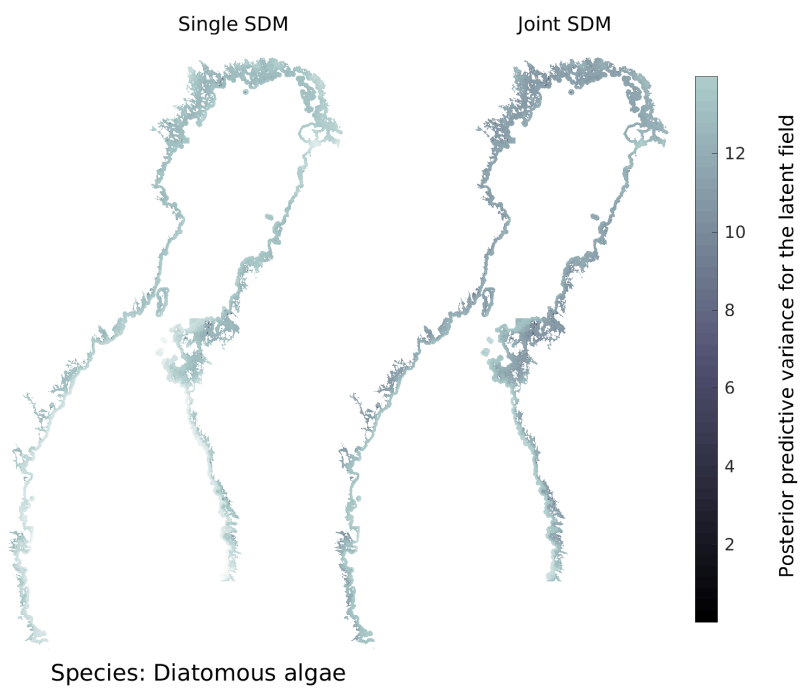


**Fig. 7.** Posterior predictive variance for the latent field  $f_*(\mathbf{x}, \mathbf{s}) | \mathbf{y}, \hat{\eta}, \hat{\lambda}$  diatomo algae.

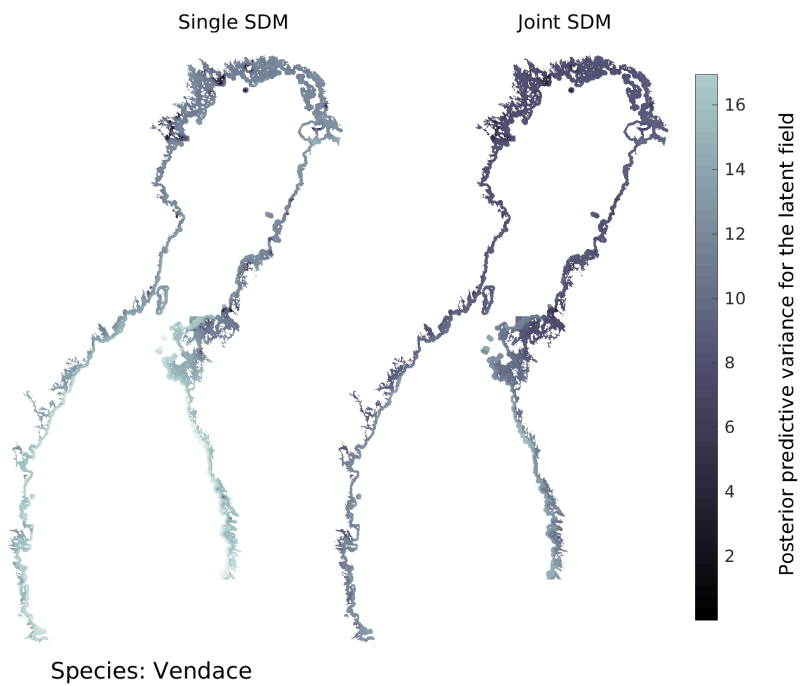


**Fig. 8.** Posterior predictive variance for the latent field  $f_*(\mathbf{x}, \mathbf{s}) | \mathbf{y}, \hat{\eta}, \hat{\lambda}$  vendace.

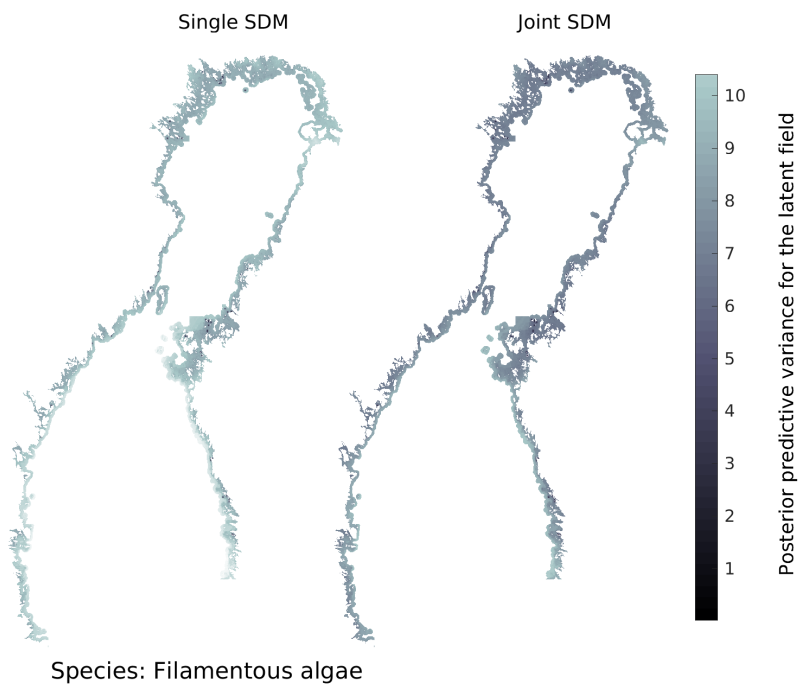


**Fig. 9.** Posterior predictive variance for the latent field  $f_*(\mathbf{x}, \mathbf{s}) | \mathbf{y}, \hat{\eta}, \hat{\lambda}$  for filamentous algae.

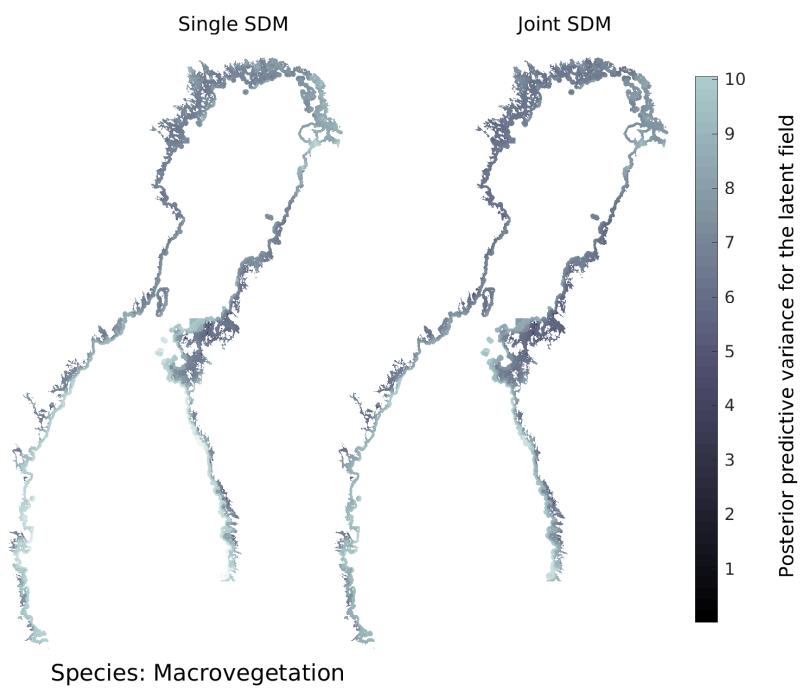


**Fig. 10.** Posterior predictive variance for the latent field  $f_*(\mathbf{x}, \mathbf{s}) | \mathbf{y}, \hat{\eta}, \hat{\lambda}$  for macrovegetation.

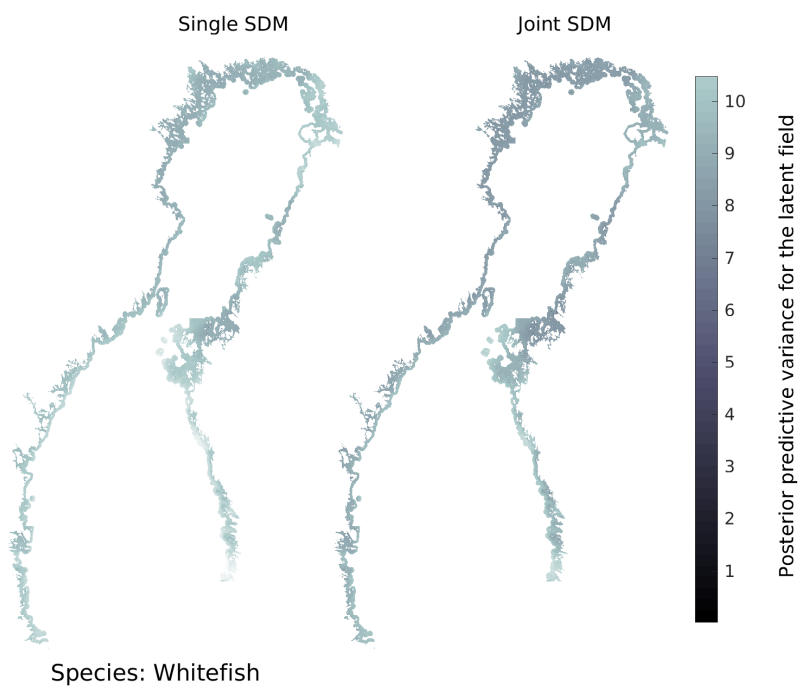


**Fig. 11.** Posterior predictive variance for the latent field  $f_*(\mathbf{x}, \mathbf{s}) | \mathbf{y}, \hat{\eta}, \hat{\lambda}$  for whitefish.

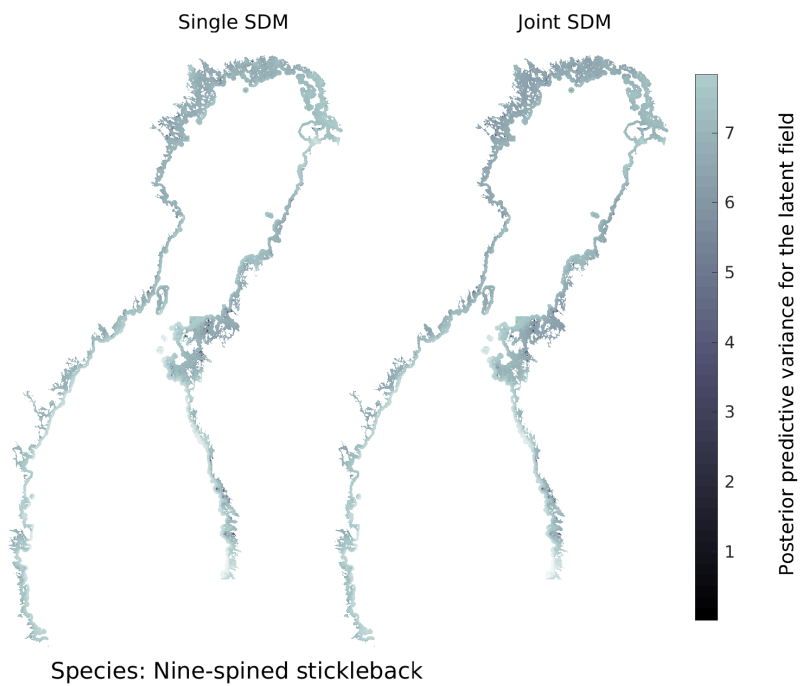


**Fig. 12.** Posterior predictive variance for the latent field  $f_*(\mathbf{x}, \mathbf{s}) | \mathbf{y}, \hat{\eta}, \hat{\lambda}$  ninespine-stickleback.

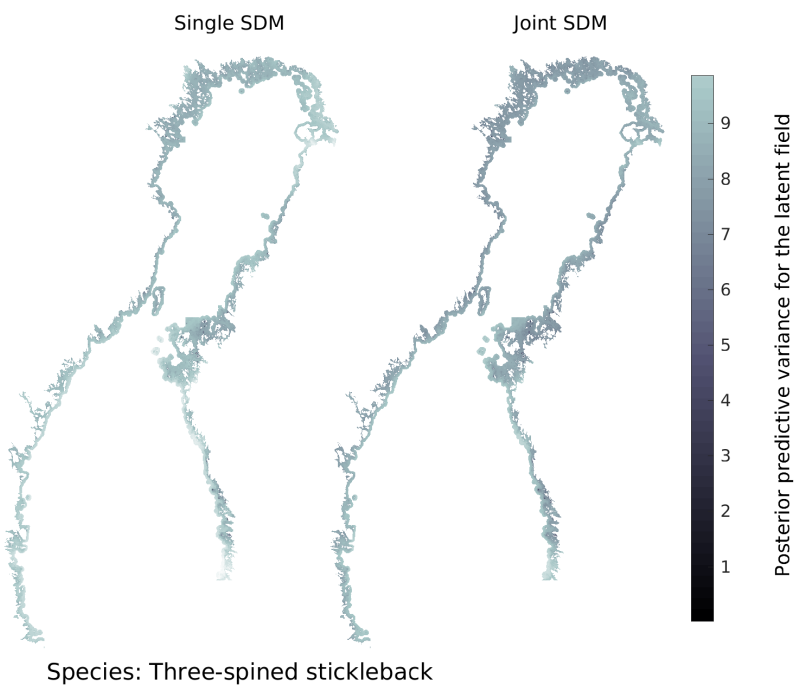


**Fig. 13.** Posterior predictive variance for the latent field  $f_*(\mathbf{x}, \mathbf{s}) | \mathbf{y}, \hat{\eta}, \hat{\lambda}$  for threespine-stickleback.